Available online at www.sciencedirect.com
ScienceDirect
Signal Processing 88 (2008) 1382–1401
SIGNAL PROCESSING
www.elsevier.com/locate/sigpro

Blind channel identification algorithms based on the Parafac decomposition of cumulant tensors: The single and multiuser cases

Carlos Estêvão R. Fernandes[a,1], Gérard Favier[a,*], João Cesar M. Mota[b]

[a]*I3S Laboratory, University of Nice Sophia Antipolis (UNSA), CNRS, 2000 route des Lucioles, 06903 Sophia Antipolis, France*
[b]*Teleinformatics Engineering Department (DETI), Federal University of Ceará (UFC), Campus do Pici, 60455-760 Fortaleza, Brazil*

Received 21 June 2007; received in revised form 30 November 2007; accepted 6 December 2007
Available online 23 December 2007

Abstract

In this paper, we exploit the symmetry properties of 4th-order cumulants to develop new blind channel identification algorithms that utilize the parallel factor (Parafac) decomposition of cumulant tensors by solving a single-step (SS) least squares (LS) problem. We first consider the case of single-input single-output (SISO) finite impulse response (FIR) channels and then we extend the results to multiple-input multiple-output (MIMO) instantaneous mixtures. Our approach is based on 4th-order output cumulants only and it is shown to hold for certain underdetermined mixtures, i.e. systems with more sources than sensors. A simplified approach using a reduced-order tensor is also discussed. Computer simulations are provided to assess the performance of the proposed algorithms in both SISO and MIMO cases, comparing them to other existing solutions. Initialization and convergence issues are also addressed.

Keywords: Channel identification; Parameter estimation; Tensor decomposition; Underdetermined linear mixtures

1. Introduction

In digital telecommunication systems, parametric channel modelling and estimation are of great importance. The knowledge of the channel model can be used to design equalizers to deconvolve the received signals. Channel identification and equalization consist in the retrieval of unknown information about the transmission channel and source signals, respectively. In order to reach a desired quality of service, broadband wireless communication systems classically perform channel identification and/or equalization using pilot symbols, i.e. training sequences composed of *a priori* known signals. This supervised approach introduces an overhead to the transmission system that may not be suitable for certain radio communication systems since it reduces the effective transmission rate. On the other hand, unsupervised (or "*blind*") approaches take only the output signals into account

*Corresponding author. Tel.: +33 492 942 736; fax: +33 492 942 896.
E-mail addresses: cfernand@i3s.unice.fr (C.E.R. Fernandes), favier@i3s.unice.fr (G. Favier), mota@deti.ufc.br (J.C.M. Mota).
[1]Supported by the CAPES agency of the Brazilian government (BEX 1488/02-3) and the contract ANR-06-BLAN-0074 "DECOTES".

0165-1684/$ - see front matter © 2007 Elsevier B.V. All rights reserved.
doi:10.1016/j.sigpro.2007.12.010

with possibly some *a priori* hypothesis on the input signals.

High-order statistics (HOS) have been an important research topic in diverse fields including data communication, speech and image processing and geophysical data processing. For stationary real signals, the second-order statistics (SOS) are not able to keep the phase information of a *nonminimum* phase system and, unless additional information about the input signal is known, the use of HOS is generally mandatory for blindly identifying finite impulse response (FIR) channels. The high-order spectra have the ability to preserve both magnitude and (nonminimum) phase information. Moreover, it is well known that all the cumulants of order greater than 2 vanish for Gaussian signals, which makes HOS-based identification methods insensitive to an additive Gaussian noise (cf. [1,2] and references therein). A vast amount of papers exist on this subject, proposing different methods that exploit high-order cumulants (cf. [3–5] among others).

Output cumulants of order higher than two can be viewed as tensors with a highly symmetrical structure [6]. Among the earliest works exploiting the cumulant symmetries with a tensor formalism, Cardoso introduced the concept of eigen-structure of 4th-order cumulant tensors [7,8]. He used the uniqueness property of the cumulant tensors as an advantage over singular value decomposition (SVD), but pre-whitening was needed. Later on, an extended Jacobi technique for approximate simultaneous diagonalization was proposed by Cardoso and Soloumiac in [9]. This latter paper introduced the JADE algorithm that uses second and 4th-order statistics to estimate an instantaneous multiple-input multiple-output (MIMO) channel in the context of blind beamforming. The joint diagonalization technique became very popular and has been used by Belouchrani et al. to propose the second-order blind identification (SOBI) algorithm [10], which uses a set of correlation matrices to identify stationary sources with different spectral contents, also in the context of instantaneous MIMO channels. On the other hand, the fourth-order system identification (FOSI) algorithm [11] treats single-input single-output (SISO) FIR channels and also involves an a priori transformation over the cumulant matrices, which is often a source of increased complexity and estimation errors. Important modifications of the technique proposed in [8] were provided by De Lathauwer et al. in [12], resorting to joint diagonalization techniques. More recently, the joint diagonalization approach has been used in [13] to propose the ICAR algorithm, which exploits the redundancies in the 4th-order cumulant to estimate the mixture matrix, but only in the overdetermined case, i.e. the case of systems with more sensors than sources. The quadricovariance is also used by the FOOBI-type algorithms proposed in [14], making use of its column-wise Kronecker structure to estimate underdetermined mixtures (more sources than sensors).

Since the introduction of the independent component analysis (ICA) concept in the seminal paper by Comon [15], research efforts have been spent for generalizing simultaneous diagonalization criteria and establishing links with canonical tensor decompositions (cf. [16,17] and references therein). For instance, in [18], De Lathauwer et. al reformulated the canonical decomposition of high-order tensors as a simultaneous generalized Schur decomposition. The Parafac analysis of a P-dimensional tensor with rank F consists in the decomposition of the tensor into a sum of F rank-one tensors, each one being written as an outer product of P vectors [19]. It is now well known that the blind identification of linear mixtures is closely related to the (simultaneous) diagonalization of symmetric cumulant tensors [20,21]. The key-point in the use of the Parafac decomposition is its uniqueness property, which can be ensured under simple conditions that are stated in the Kruskal Theorem [22]. Furthermore, canonical tensor decompositions do not impose any kind of orthogonality constraints and the factorization of tensors composed of high-order output cumulants has the advantage of avoiding the so-called *pre-whitening* operation by fully exploiting the multidimensional nature of the cumulant tensor. Moreover, the tensor rank is not bounded by the tensor dimensions as it is the case for matrices, which conceptually allows for the blind identification of underdetermined mixtures. Actually, this problem has received a special attention from the signal processing community under different tensor approaches that include, among others, the decomposition of *quantics* in sums of powers of linear forms [23]; the use of congruent transformation [24] exploiting the virtual array concept [25,26]; and the use of high-order derivatives of the multivariate characteristic function [27]. Besides, a frequency domain framework for MIMO system identification using Parafac was introduced in [28] using HOS-based tensors. More recently, that approach was further developed including the underdetermined case [29–31].

A formal relationship between Parafac decomposition and simultaneous matrix diagonalization has been established in [32] showing that the components of the tensor decomposition can be obtained from a simultaneous matrix diagonalization by congruence transformation, leading to weaker uniqueness conditions. These ideas gave rise to the FOOBI algorithms [14], which are theoretically able to identify a greater number of user channels for a given number of receive antennas. The approach used by the ICAR method [13] can also include the case of underdetermined mixtures, resorting to 6th- [33] or higher-order statistics [24]. These latter papers propose methods avoiding prewhitening, but still breaking the problem into two optimization procedures, which remains necessary to extract the MIMO channel coefficients from an initial estimate based on an eigenvalue decomposition (EVD).

Several algorithms propose solutions to fit a Pth-order Parafac model. The well-known alternating least squares (ALS) algorithm iteratively minimizes, in an alternate way, P least squares (LS) cost functions. Our main focus in this paper is to exploit the redundancies of the factors of the 4th-order cumulant tensor decomposition in the minimization problem in order to develop new single-step (SS) LS Parafac-based Blind Channel Identification (SS-LS PBCI) algorithms. This approach is completely different from the previously cited ones, since it proposes to estimate the channel coefficients by searching the solution of a single minimization problem, under very mild assumptions. In addition, we treat both the convolutive SISO and instantaneous MIMO cases using the same underlying idea. In the former case, the proposed approach constitutes a new scheme for the estimation of FIR systems. In the MIMO case, this paper seems to be the first one to account for the redundancies contained in the factors of the Parafac decomposition of the cumulant tensor in the LS minimization problem.

In the sequel, we will be first interested in recovering the impulse response of a complex-valued SISO-FIR channel from the Parafac decomposition of a 3rd-order tensor composed of 4th-order output cumulants. Using our SS approach, the permutation and scaling ambiguities intrinsic to the Parafac decomposition are solved and the uniqueness issue is addressed. After that, we consider the problem of blind MIMO channel (mixture) identification in the context of a multiuser system characterized by instantaneous complex-valued channels. We describe our SS-LS Parafac-based blind MIMO channel identification (SS-LS PBMCI) algorithms, based on the decomposition of 4th- and 3rd-order tensors composed of 4th-order spatial cumulants. Although our main goal is not the estimation of underdetermined mixtures, we make use of some tensor properties to show that under certain conditions our algorithms are able to identify channels with more sources than sensors. Computer simulations illustrate the performance gains that our method provides with respect to other existing solutions. We also assess the algorithms performances by recovering the input signals using a minimum mean squared error (MMSE) equalizer built from the estimated channel. In the MIMO case, we build a *semi-blind* MMSE equalizer using a few pilot symbols.

The rest of this paper is organized as follows. In Section 2, we present a review of the Parafac decomposition with a brief description of the quadrilinear and trilinear versions of the ALS algorithm; in Section 3, we introduce the SISO signal model and express the tensor of output cumulants as a Parafac model; in Section 4, we give the equations describing our cumulant tensor decomposition, establishing a link between our method and the (joint) matrix diagonalization approach; we then introduce our Parafac-based algorithm to estimate the channel parameters based on a SS-LS minimization procedure; our approach is extended to the multiuser and multi-antenna case in Sections 5 and 6; Section 7 presents some computer simulation results to illustrate the proposed identification methods and, finally we draw some conclusions and discuss perspectives in Section 8.

Notations and definitions:

$(\cdot)^*$	the conjugate operation
$(\cdot)^{\mathsf{T}}$	the transpose operation
$(\cdot)^{\mathsf{H}}$	the conjugate transpose (*Hermitian*)
$\mathbf{I}_n$	the $n \times n$ identity matrix
$(\cdot)^{\#}$	the *Moore–Penrose* pseudoinverse, defined for a full-rank $m \times n$ matrix $\mathbf{X} \in \mathbb{C}^{m \times n}$ as $\mathbf{X}^{\#} = (\mathbf{X}^{\mathsf{H}}\mathbf{X})^{-1}\mathbf{X}^{\mathsf{H}}$ if $m \geqslant n$, $\mathbf{X}^{\#} = \mathbf{X}^{\mathsf{H}}(\mathbf{X}\mathbf{X}^{\mathsf{H}})^{-1}$ otherwise
$\mathrm{Diag}(\cdot)$	a diagonal matrix built from the entries of the vector argument
$D_i(\cdot)$	a diagonal matrix built from the ith row of the matrix argument

$\mathbf{X}_{\cdot i}$ the ith column of an $m \times n$ matrix $\mathbf{X}$, i.e. $\mathbf{X} = [\mathbf{X}_{\cdot 1} \dots \mathbf{X}_{\cdot n}]$

$\underline{\mathbf{x}}$ normalized vector i.e. $\underline{\mathbf{x}} = \mathbf{x}/(\mathbf{x}^{\mathsf{H}}\mathbf{x})^{1/2}$. For an $m \times n$ matrix $\mathbf{X}$ we have $\underline{\mathbf{X}} = [\underline{\mathbf{X}}_{\cdot 1} \dots \underline{\mathbf{X}}_{\cdot n}]$

vec$(\cdot)$ the *vectorization* operator: stacks the columns of its matrix argument into a column vector

$\circ$ the outer product

$\otimes$ the Kronecker product

$\diamond$ the Khatri–Rao product. For matrices $\mathbf{X}$ and $\mathbf{Y}$ of dimensions $m \times q$ and $n \times q$, respectively, the Khatri–Rao product is defined as follows:

$$\mathbf{X} \diamond \mathbf{Y} \triangleq [\mathbf{X}_{\cdot 1} \otimes \mathbf{Y}_{\cdot 1} \dots \mathbf{X}_{\cdot q} \otimes \mathbf{Y}_{\cdot q}] = \begin{pmatrix} \mathbf{Y}D_1(\mathbf{X}) \\ \vdots \\ \mathbf{Y}D_m(\mathbf{X}) \end{pmatrix} \in \mathbb{C}^{mn \times q},$$

The following property of the Khatri–Rao product will be used [34,35]:

Property 1. *If* $\mathbf{Z} = \mathbf{X}\mathrm{Diag}(\mathbf{v})\mathbf{Y}$, *where* $\mathbf{X} \in \mathbb{C}^{m \times q}$, $\mathbf{Y} \in \mathbb{C}^{q \times n}$ *and* $\mathbf{v} \in \mathbb{C}^{q \times 1}$, *then it holds*:

$$\mathrm{vec}(\mathbf{Z}) = (\mathbf{Y}^{\mathsf{T}} \diamond \mathbf{X})\mathbf{v} \in \mathbb{C}^{mn \times 1}. \quad \text{(P-1)}$$

2. Parafac tensor decomposition

The Parafac analysis of a P-dimensional tensor with rank F consists in the decomposition of the tensor into a sum of F rank-one tensors, each one being written as an outer product of P vectors [19]. The *trilinear* Parafac model ($P = 3$) has become very popular in the fields of Psychometrics and Chemometrics [36,37] and also has been widely used in signal processing applications (cf. [38,23,39] among others).

Let us consider the Pth-order tensor $\mathscr{T}^{(P)}$ of dimensions $I_1 \times \cdots \times I_P$ having the following F-component decomposition:

$$t_{i_1 \dots i_P} = \sum_{f=1}^{F} a^{(1)}_{i_1 f} \dots a^{(P)}_{i_P f}, \quad (1)$$

where $i_p \in [1, I_p]$, with $p \in [1, P]$. The sum expressed in (1) is the scalar representation of the Parafac decomposition of tensor $\mathscr{T}^{(P)}$. The rank of a tensor is defined as the minimum number F of factors needed to decompose it in the form (1). The tensor $\mathscr{T}^{(P)}$ can be written as the sum of F outer products[2] involving P vectors, as follows:

$$\mathscr{T}^{(P)} = \sum_{i_1=1}^{I_1} \cdots \sum_{i_P=1}^{I_P} t_{i_1 \dots i_P} \mathbf{e}^{(I_1)}_{i_1} \circ \cdots \circ \mathbf{e}^{(I_P)}_{i_P} = \sum_{f=1}^{F} \mathbf{A}^{(1)}_{\cdot f} \circ \cdots \circ \mathbf{A}^{(P)}_{\cdot f}, \quad (2)$$

where $\circ$ is the outer product and the notation $\mathbf{e}^{(I_p)}_{i_p}$ stands for the i_pth canonical basis vector of $\mathbb{R}^{I_p}$, $i_p \in [1, I_p]$, $p \in [1, P]$, and $\mathbf{A}^{(p)}_{\cdot f} = \sum_{i_p=1}^{I_p} a^{(p)}_{i_p f} \mathbf{e}^{(I_p)}_{i_p}$, $f \in [1, F]$, corresponds to the fth column of matrix $\mathbf{A}^{(p)}$, with dimensions $I_p \times F$. The P matrices $\mathbf{A}^{(p)}$ with elements $a^{(p)}_{i_p f}$ contain all the tensor information and will be referred to as the loading factors. We define a d-dimensional *slice* of tensor $\mathscr{T}^{(P)}$ as the set of elements obtained by freezing $P - d$ of its P indexes and making the d other ones to vary in their respective ranges. As a result, *one-dimensional* (1D) tensor slices can be viewed as vectors and *two-dimensional* (2D) tensor slices are matrices.

The main property of Parafac is its uniqueness for tensors of order higher than 2. The Parafac decomposition of a tensor $\mathscr{T}^{(P)}$ with loading factors $\{\mathbf{A}^{(1)}, \dots, \mathbf{A}^{(P)}\}$ is said to be essentially unique if any other set $\{\bar{\mathbf{A}}^{(1)}, \dots, \bar{\mathbf{A}}^{(P)}\}$ satisfying the Parafac decomposition (1) is such that

$$\bar{\mathbf{A}}^{(p)} = \mathbf{A}^{(p)}\mathbf{\Lambda}_p\mathbf{\Pi}, \quad \forall p \in [1, P], \quad (3)$$

where $\mathbf{\Pi}$ is a permutation matrix and $\mathbf{\Lambda}_p$, $p \in [1, P]$, are diagonal scaling matrices satisfying $\prod_{p=1}^{P} \mathbf{\Lambda}_p = \mathbf{I}_F$ [40]. A sufficient uniqueness condition was stated by Kruskal in [22] for the case of a 3rd-order tensor. Sidiropoulos and Bro extended the Kruskal Theorem to the case of Pth-order tensors, as follows [37]:

Theorem 1. *The Parafac decomposition of a Pth-order tensor with rank* $F > 1$, *is essentially unique* (*up to column scaling and permutation*) *if*

$$\sum_{p=1}^{P} k_{A^{(p)}} \geqslant 2F + (P - 1), \quad (4)$$

where $k_{A^{(p)}}$ *denotes the k-rank of the loading factor* $\mathbf{A}^{(p)}$, $p \in [1, P]$.

[2] The outer product of two arrays $\mathscr{A}^{(P)} \in \mathbb{C}^{I_1 \times \cdots \times I_P}$ and $\mathscr{B}^{(Q)} \in \mathbb{C}^{J_1 \times J_1 \times \cdots \times J_Q}$ consists of a tensor of order $P + Q$ in which the element in position $i_1, i_2, \dots, i_P, j_1, j_2, \dots, j_Q$ equals the product $a_{i_1 i_2 \dots i_P} b_{j_1 j_2 \dots j_Q}$.

Table 1
Parafac formulae for a 4th-order tensor $\mathscr{T}^{(4)}$

Planes	2D slices	(dim.)	Unfolded matrices	(dim.)
$l \times i$	$\mathbf{T}_{\cdot jk\cdot} = \mathbf{A}^{(4)} D_j(\mathbf{A}^{(2)}) D_k(\mathbf{A}^{(3)}) \mathbf{A}^{(1)\mathsf{T}}$	$L \times I$	$\mathbf{T}_{[2,3]} = (\mathbf{A}^{(2)} \diamond \mathbf{A}^{(3)} \diamond \mathbf{A}^{(4)}) \mathbf{A}^{(1)\mathsf{T}}$	$JKL \times I$
$i \times j$	$\mathbf{T}_{\cdot\cdot kl} = \mathbf{A}^{(1)} D_k(\mathbf{A}^{(3)}) D_l(\mathbf{A}^{(4)}) \mathbf{A}^{(2)\mathsf{T}}$	$I \times J$	$\mathbf{T}_{[3,4]} = (\mathbf{A}^{(3)} \diamond \mathbf{A}^{(4)} \diamond \mathbf{A}^{(1)}) \mathbf{A}^{(2)\mathsf{T}}$	$KLI \times J$
$j \times k$	$\mathbf{T}_{i\cdot\cdot l} = \mathbf{A}^{(2)} D_l(\mathbf{A}^{(4)}) D_i(\mathbf{A}^{(1)}) \mathbf{A}^{(3)\mathsf{T}}$	$J \times K$	$\mathbf{T}_{[4,1]} = (\mathbf{A}^{(4)} \diamond \mathbf{A}^{(1)} \diamond \mathbf{A}^{(2)}) \mathbf{A}^{(3)\mathsf{T}}$	$LIJ \times K$
$k \times l$	$\mathbf{T}_{ij\cdot\cdot} = \mathbf{A}^{(3)} D_i(\mathbf{A}^{(1)}) D_j(\mathbf{A}^{(2)}) \mathbf{A}^{(4)\mathsf{T}}$	$K \times L$	$\mathbf{T}_{[1,2]} = (\mathbf{A}^{(1)} \diamond \mathbf{A}^{(2)} \diamond \mathbf{A}^{(3)}) \mathbf{A}^{(4)\mathsf{T}}$	$IJK \times L$

The k-rank of an $m \times n$ matrix $\mathbf{X}$ equals the largest integer k_X such that *any* set of k_X columns of $\mathbf{X}$ is independent. From this definition, we notice that $k_X \leqslant r_X \leqslant \min(m,n)$, where $r_X = \operatorname{rank}(\mathbf{X})$. Several authors have addressed the Parafac uniqueness problem and different proofs have been given to the Kruskal Theorem [22,37,41]. Uniqueness represents a great advantage of Parafac over matrix decompositions, since Parafac does not produce rotational ambiguities. In addition, there are no orthogonality constraints such as in SVD, even in the symmetric case where such constraints also apply to EVD.

Let us consider a 4th-order tensor $\mathscr{T}^{(4)}$ of dimensions $I \times J \times K \times L$ with elements $t_{ijkl} = \sum_{f=1}^{F} a_{if}^{(1)} a_{jf}^{(2)} a_{kf}^{(3)} a_{lf}^{(4)}$, where $i \in [1, I]$, $j \in [1, J]$, $k \in [1, K]$ and $l \in [1, L]$. In order to obtain 2D slices of tensor $\mathscr{T}^{(4)}$, we fix a pair of indexes (n_1, n_2), $n_1, n_2 \in \{i, j, k, l\}$, thus defining a plane along two dimensions of the tensor. For instance, freezing the third and fourth indexes (k, l) in t_{ijkl}, we get the 2D slices along the plane $i \times j$, which form a set of KL matrices $\mathbf{T}_{\cdot\cdot k\, l}$, with dimensions $I \times J$, as follows:

$$\begin{aligned}\mathbf{T}_{\cdot\cdot k\, l} &= \sum_{i=1}^{I} \sum_{j=1}^{J} t_{ijkl} \mathbf{e}_i^{(I)} \mathbf{e}_j^{(J)\mathsf{T}} = \sum_{f=1}^{F} a_{kf}^{(3)} a_{lf}^{(4)} \mathbf{A}_{\cdot f}^{(1)} \mathbf{A}_{\cdot f}^{(2)\mathsf{T}} \\ &= \mathbf{A}^{(1)} D_k(\mathbf{A}^{(3)}) D_l(\mathbf{A}^{(4)}) \mathbf{A}^{(2)\mathsf{T}}, \quad k \in [1, K], \\ &\quad l \in [1, L], \end{aligned} \tag{5}$$

where $\mathbf{A}^{(1)} \in \mathbb{C}^{I \times F}$, $\mathbf{A}^{(2)} \in \mathbb{C}^{J \times F}$, $\mathbf{A}^{(3)} \in \mathbb{C}^{K \times F}$ and $\mathbf{A}^{(4)} \in \mathbb{C}^{L \times F}$ are the loading factors with elements $a_{if}^{(1)}$, $a_{jf}^{(2)}$, $a_{kf}^{(3)}$ and $a_{lf}^{(4)}$, respectively. Stacking the slices $\mathbf{T}_{\cdot\cdot kl}$, $l \in [1, L]$, for a given fixed k we have $\mathbf{T}_{[4]_k} = [\mathbf{T}_{\cdot\cdot k1}^{\mathsf{T}} \cdots \mathbf{T}_{\cdot\cdot kL}^{\mathsf{T}}]^{\mathsf{T}} \in \mathbb{C}^{LI \times J}$, $k \in [1, K]$.

Using (5) we get

$$\begin{aligned}\mathbf{T}_{[4]_k} &= [D_1(\mathbf{A}^{(4)}) D_k(\mathbf{A}^{(3)}) \mathbf{A}^{(1)\mathsf{T}} \\ &\quad \cdots D_L(\mathbf{A}^{(4)}) D_k(\mathbf{A}^{(3)}) \mathbf{A}^{(1)\mathsf{T}}]^{\mathsf{T}} \mathbf{A}^{(2)\mathsf{T}} \\ &= [\mathbf{A}^{(4)} \diamond (\mathbf{A}^{(1)} D_k(\mathbf{A}^{(3)}))] \mathbf{A}^{(2)\mathsf{T}}\end{aligned}$$

Stacking the matrices $\mathbf{T}_{[4]_k}$ for $k \in [1, K]$, we get an unfolded representation of tensor $\mathscr{T}^{(4)}$, as follows:

$$\begin{aligned}\mathbf{T}_{[3,4]} &= \begin{pmatrix} \mathbf{T}_{[4]_1} \\ \vdots \\ \mathbf{T}_{[4]_K} \end{pmatrix} = \begin{pmatrix} \mathbf{A}^{(4)} \diamond \mathbf{A}^{(1)} D_1(\mathbf{A}^{(3)}) \\ \vdots \\ \mathbf{A}^{(4)} \diamond \mathbf{A}^{(1)} D_K(\mathbf{A}^{(3)}) \end{pmatrix} \mathbf{A}^{(2)\mathsf{T}} \\ &= (\mathbf{A}^{(3)} \diamond \mathbf{A}^{(4)} \diamond \mathbf{A}^{(1)}) \mathbf{A}^{(2)\mathsf{T}} \in \mathbb{C}^{KLI \times J}, \end{aligned} \tag{6}$$

where the notation $\mathbf{T}_{[3,4]}$ indicates that the third index, k, varies more slowly than the fourth index, l. Besides plane $i \times j$, there exist five other *slicing planes* for a 4th-order tensor. However, for the purpose of estimating the loading matrices, we only need four unfolded representations. Table 1 summarizes the 4th-order Parafac formulae, including tensor slices, unfolded representations and their respective dimensions. Other slicing planes are omitted since they will not be used.

For $P = 3$, slicing tensor $\mathscr{T}^{(3)}$ along each of its three dimensions leads to horizontal, vertical and frontal slices. The expressions for these matrices are given in Table 2 with their corresponding unfolded representations $\mathbf{T}_{[1]}$, $\mathbf{T}_{[2]}$ and $\mathbf{T}_{[3]}$.

Algorithms

To estimate the loading factors of the Parafac model, we will be particularly interested in cumulant-matching approaches based on the use of ALS-type algorithms. In the case of a Pth-order tensor, the basic idea is to estimate each loading factor by iteratively minimizing P LS cost functions, conditioned to previous estimates of $P - 1$ factors. The algorithm iterates until no improvements are observed (cf. [42] and references therein). Main drawbacks include possible slow convergence and/or convergence to local minima due to inadequate initializations.

Table 2
Parafac formulae for a 3rd-order tensor $\mathscr{T}^{(3)}$

Slicing directions	2D slices	(dim.)	Unfolded matrices	(dim.)
Horizontal (i)	$\mathbf{T}_{i\cdot\cdot} = \mathbf{A}^{(2)} D_i(\mathbf{A}^{(1)})\mathbf{A}^{(3)\mathsf{T}}$	$(J \times K)$	$\mathbf{T}_{[1]} = (\mathbf{A}^{(1)} \diamond \mathbf{A}^{(2)})\mathbf{A}^{(3)\mathsf{T}}$	$(IJ \times K)$
Vertical (j)	$\mathbf{T}_{\cdot j\cdot} = \mathbf{A}^{(3)} D_j(\mathbf{A}^{(2)})\mathbf{A}^{(1)\mathsf{T}}$	$(K \times I)$	$\mathbf{T}_{[2]} = (\mathbf{A}^{(2)} \diamond \mathbf{A}^{(3)})\mathbf{A}^{(1)\mathsf{T}}$	$(JK \times I)$
Frontal(k)	$\mathbf{T}_{\cdot\cdot k} = \mathbf{A}^{(1)} D_k(\mathbf{A}^{(3)})\mathbf{A}^{(2)\mathsf{T}}$	$(I \times J)$	$\mathbf{T}_{[3]} = (\mathbf{A}^{(3)} \diamond \mathbf{A}^{(1)})\mathbf{A}^{(2)\mathsf{T}}$	$(KI \times J)$

Quadrilinear ALS algorithm. For a 4th-order tensor $\mathscr{T}^{(4)}$, the matrices $\{\mathbf{A}^{(1)}, \mathbf{A}^{(2)}, \mathbf{A}^{(3)}, \mathbf{A}^{(4)}\}$ are estimated by minimizing, in an alternate way, the four following LS criteria, deduced from Table 1:

$$\psi_1(\hat{\mathbf{A}}^{(2)}_{r-1}, \hat{\mathbf{A}}^{(3)}_{r-1}, \hat{\mathbf{A}}^{(4)}_{r-1}, \mathbf{A}^{(1)}) = \|\mathbf{T}_{[2,3]} - (\hat{\mathbf{A}}^{(2)}_{r-1} \diamond \hat{\mathbf{A}}^{(3)}_{r-1} \diamond \hat{\mathbf{A}}^{(4)}_{r-1})\mathbf{A}^{(1)\mathsf{T}}\|^2_{\mathrm{F}},$$

$$\psi_2(\hat{\mathbf{A}}^{(1)}_{r}, \hat{\mathbf{A}}^{(3)}_{r-1}, \hat{\mathbf{A}}^{(4)}_{r-1}, \mathbf{A}^{(2)}) = \|\mathbf{T}_{[3,4]} - (\hat{\mathbf{A}}^{(3)}_{r-1} \diamond \hat{\mathbf{A}}^{(4)}_{r-1} \diamond \hat{\mathbf{A}}^{(1)}_{r})\mathbf{A}^{(2)\mathsf{T}}\|^2_{\mathrm{F}},$$

$$\psi_3(\hat{\mathbf{A}}^{(1)}_{r}, \hat{\mathbf{A}}^{(2)}_{r}, \hat{\mathbf{A}}^{(4)}_{r-1}, \mathbf{A}^{(3)}) = \|\mathbf{T}_{[4,1]} - (\hat{\mathbf{A}}^{(4)}_{r-1} \diamond \hat{\mathbf{A}}^{(1)}_{r} \diamond \hat{\mathbf{A}}^{(2)}_{r})\mathbf{A}^{(3)\mathsf{T}}\|^2_{\mathrm{F}},$$

$$\psi_4(\hat{\mathbf{A}}^{(1)}_{r}, \hat{\mathbf{A}}^{(2)}_{r}, \hat{\mathbf{A}}^{(3)}_{r}, \mathbf{A}^{(4)}) = \|\mathbf{T}_{[1,2]} - (\hat{\mathbf{A}}^{(1)}_{r} \diamond \hat{\mathbf{A}}^{(2)}_{r} \diamond \hat{\mathbf{A}}^{(3)}_{r})\mathbf{A}^{(4)\mathsf{T}}\|^2_{\mathrm{F}},$$

where r stands for the iteration number and $\|\cdot\|_{\mathrm{F}}$ denotes the Frobenius norm. Each loading factor is updated by fixing the three other ones to their previously estimated values. The solutions are obtained from classical LS minimization. Matrix $\mathbf{A}^{(1)}$, for instance, can be estimated as follows:

$$\begin{aligned}\hat{\mathbf{A}}^{(1)\mathsf{T}}_{r} &= \arg\min_{\mathbf{A}^{(1)}}\{\psi_1(\hat{\mathbf{A}}^{(2)}_{r-1}, \hat{\mathbf{A}}^{(3)}_{r-1}, \hat{\mathbf{A}}^{(4)}_{r-1}, \mathbf{A}^{(1)})\} \\ &= (\hat{\mathbf{A}}^{(2)}_{r-1} \diamond \hat{\mathbf{A}}^{(3)}_{r-1} \diamond \hat{\mathbf{A}}^{(4)}_{r-1})^{\#}\mathbf{T}_{[2,3]}. \end{aligned} \quad (7)$$

The initial guesses $\hat{\mathbf{A}}^{(2)}_0$, $\hat{\mathbf{A}}^{(3)}_0$ and $\hat{\mathbf{A}}^{(4)}_0$ may be chosen as Gaussian random matrices, though this is not necessarily the best choice [42]. Similar expressions can be obtained for $\hat{\mathbf{A}}^{(2)}_r$, $\hat{\mathbf{A}}^{(3)}_r$ and $\hat{\mathbf{A}}^{(4)}_r$.

The algorithm can be summarized as follows: at each iteration $r \geqslant 1$, using the preceding estimates $\hat{\mathbf{A}}^{(2)}_{r-1}$, $\hat{\mathbf{A}}^{(3)}_{r-1}$ and $\hat{\mathbf{A}}^{(4)}_{r-1}$ we compute $\hat{\mathbf{A}}^{(1)}_r$ by means of (7). Then, taking $\hat{\mathbf{A}}^{(1)}_r$ into account and still using $\hat{\mathbf{A}}^{(3)}_{r-1}$ and $\hat{\mathbf{A}}^{(4)}_{r-1}$, we estimate $\hat{\mathbf{A}}^{(2)}_r$ from the minimization of ψ_2. After that, $\hat{\mathbf{A}}^{(3)}_r$ is obtained by minimizing ψ_3 using the current estimates $\hat{\mathbf{A}}^{(1)}_r$ and $\hat{\mathbf{A}}^{(2)}_r$ as well as $\hat{\mathbf{A}}^{(4)}_{r-1}$. Finally, $\hat{\mathbf{A}}^{(4)}_r$ is estimated from ψ_4 using $\hat{\mathbf{A}}^{(1)}_r$, $\hat{\mathbf{A}}^{(2)}_r$ and $\hat{\mathbf{A}}^{(3)}_r$. The algorithm iterates until the difference between the measured tensor and the tensor reconstructed using the estimated loading factors does not significantly change between two successive iterations. The above described procedure will be referred to as the quadrilinear Parafac-ALS (QALS) algorithm.

Trilinear ALS algorithm. A similar ALS approach can be applied to a 3rd-order tensor $\mathscr{T}^{(3)}$. Using the expressions in Table 2, the loading factors $\mathbf{A}^{(1)}$, $\mathbf{A}^{(2)}$ and $\mathbf{A}^{(3)}$ are estimated by minimizing the three following LS criteria, in an alternate way

$$\psi_1(\hat{\mathbf{A}}^{(2)}_{r-1}, \hat{\mathbf{A}}^{(3)}_{r-1}, \mathbf{A}^{(1)}) = \|\mathbf{T}_{[2]} - (\hat{\mathbf{A}}^{(2)}_{r-1} \diamond \hat{\mathbf{A}}^{(3)}_{r-1})\mathbf{A}^{(1)\mathsf{T}}\|^2_{\mathrm{F}},$$

$$\psi_2(\hat{\mathbf{A}}^{(1)}_{r}, \hat{\mathbf{A}}^{(3)}_{r-1}, \mathbf{A}^{(2)}) = \|\mathbf{T}_{[3]} - (\hat{\mathbf{A}}^{(3)}_{r-1} \diamond \hat{\mathbf{A}}^{(1)}_{r})\mathbf{A}^{(2)\mathsf{T}}\|^2_{\mathrm{F}},$$

$$\psi_3(\hat{\mathbf{A}}^{(1)}_{r}, \hat{\mathbf{A}}^{(2)}_{r}, \mathbf{A}^{(3)}) = \|\mathbf{T}_{[1]} - (\hat{\mathbf{A}}^{(1)}_{r} \diamond \hat{\mathbf{A}}^{(2)}_{r})\mathbf{A}^{(3)\mathsf{T}}\|^2_{\mathrm{F}}.$$

For instance, the estimation of matrix $\mathbf{A}^{(1)}$ is given by

$$\begin{aligned}\hat{\mathbf{A}}^{(1)\mathsf{T}}_{r} &= \arg\min_{\mathbf{A}^{(1)}}\{\psi_1(\hat{\mathbf{A}}^{(2)}_{r-1}, \hat{\mathbf{A}}^{(3)}_{r-1}, \mathbf{A}^{(1)})\} \\ &= (\hat{\mathbf{A}}^{(2)}_{r-1} \diamond \hat{\mathbf{A}}^{(3)}_{r-1})^{\#}\mathbf{T}_{[2]}. \end{aligned} \quad (8)$$

At each iteration, we successively update the three loading factors by fixing the two other ones to their previous estimated values. This method will be called the Trilinear Parafac-ALS (TALS) algorithm. As for the QALS algorithm, the TALS algorithm is stopped when the difference between the measured tensor and the reconstructed one converges.

3. SISO channel model and 4th-order output cumulants

Let us consider a SISO-FIR communication channel for which the output signal $y(n)$, after

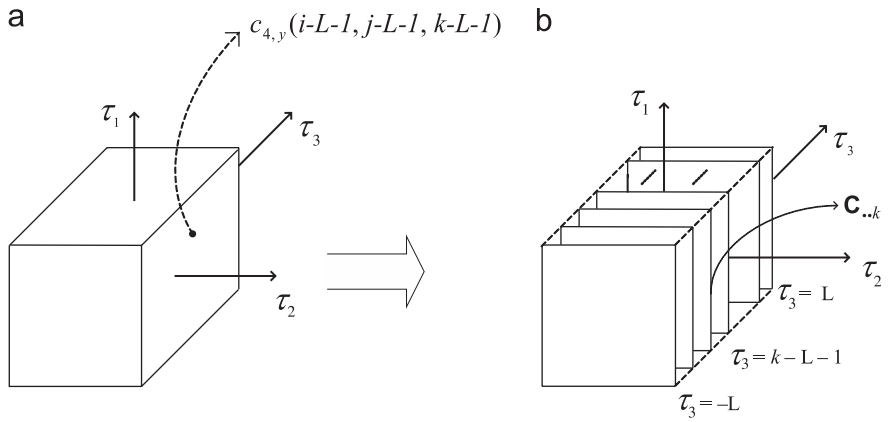

Fig. 1. (a) Three-dimensional tensor $\mathscr{C}^{(3,y)}$ of 4th-order output cumulants; (b) frontal slices of tensor $\mathscr{C}^{(3,y)}$.

sampling at the symbol rate, is written as follows:

$$y(n) = x(n) + \upsilon(n),$$

$$x(n) = \sum_{l=0}^{L} h_l s(n-l), \tag{9}$$

with $h_0 = 1$, which is equivalent to a simple unit-norm constraint. Moreover, the following assumptions are made:

A1. The non-measurable, complex-valued, discrete input sequence $s(n)$ is stationary, ergodic, independent and identically distributed (iid) with symmetric distribution, zero-mean and non-zero kurtosis $\gamma_{4,s}$, assumed to be known.

A2. The additive Gaussian noise sequence $\upsilon(n)$ is zero-mean with unknown variance σ_υ^2 and unknown autocorrelation function. It is assumed to be independent from the input signal $s(n)$.

A3. The channel frequency-response is $H(\omega) = \sum_l h_l \mathrm{e}^{-\mathrm{j}\omega l}$ with complex coefficients h_l representing the equivalent discrete impulse response, including the pulse shaping filter, the channel itself and the receiving filter.

A4. The FIR filter with impulse response $\{h_l\}$ is assumed to be causal with memory L, i.e. $h_l = 0$, $\forall l \notin [0, L]$, $h_L \neq 0$ and $L \neq 0$.

The 4th-order cumulants of the output signal $y(n)$ are defined as follows:

$$c_{4,y}(\tau_1, \tau_2, \tau_3) \triangleq \mathrm{cum}[y^*(n), y(n+\tau_1), y^*(n+\tau_2), y(n+\tau_3)]. \tag{10}$$

Using the channel model (9), taking assumptions A1 and A2 into account and making use of the multilinearity property of cumulants, we get [43]

$$c_{4,y}(\tau_1, \tau_2, \tau_3) = \gamma_{4,s} \sum_{l=0}^{L} h_l^* h_{l+\tau_1} h_{l+\tau_2}^* h_{l+\tau_3}, \tag{11}$$

where $\gamma_{4,s} = c_{4,s}(0,0,0)$. From assumption A4, we deduce that

$$c_{4,y}(\tau_1, \tau_2, \tau_3) = 0, \quad \forall |\tau_1|, |\tau_2|, |\tau_3| > L. \tag{12}$$

Hence, making the time-lags τ_1, τ_2 and τ_3 vary in the interval $[-L, L]$, we have all the possible nonzero values of $c_{4,y}(\tau_1, \tau_2, \tau_3)$. Such a choice induces a maximum redundancy in our information model.

Let us define the 3rd-order tensor $\mathscr{C}^{(3,y)} \in \mathbb{C}^{(2L+1)\times(2L+1)\times(2L+1)}$ containing all the 4th-order output cumulants, as follows:

$$\mathscr{C}^{(3,y)} = \sum_{i=1}^{2L+1} \sum_{j=1}^{2L+1} \sum_{k=1}^{2L+1} c_{ijk} \mathbf{e}_i^{(2L+1)} \circ \mathbf{e}_j^{(2L+1)} \circ \mathbf{e}_k^{(2L+1)}, \tag{13}$$

where the element in position (i, j, k) corresponds to $c_{ijk} = c_{4,y}(i - L - 1, j - L - 1, k - L - 1)$ as shown in Fig. 1a. Replacing (11) into (13), we can write the tensor $\mathscr{C}^{(3,y)}$ as a sum of $L + 1$ outer products, each one involving 3 vectors, as follows:

$$\mathscr{C}^{(3,y)} = \gamma_{4,s} \sum_{l=0}^{L} h_l^* \mathbf{H}_{\cdot l+1} \circ \mathbf{H}_{\cdot l+1}^* \circ \mathbf{H}_{\cdot l+1}, \tag{14}$$

where $\mathbf{H}_{\cdot l+1} = \sum_{p=1}^{2L+1} h_{l+p-L-1} \mathbf{e}_p^{(2L+1)}$. Eq. (14) represents the Parafac decomposition of the tensor $\mathscr{C}^{(3,y)}$. Let us define the channel coefficient matrix

$\mathbf{H} \in \mathbb{C}^{(2L+1)\times(L+1)}$ as follows:

$$\mathbf{H} \triangleq \mathscr{H}(\mathbf{h}) = [\mathbf{H}_{.1}\mathbf{H}_{.2}\dots\mathbf{H}_{.L+1}] = \begin{pmatrix} 0 & 0 & \cdots & h_0 \\ \vdots & \vdots & \ddots & \vdots \\ 0 & h_0 & \cdots & h_{L-1} \\ h_0 & h_1 & \cdots & h_L \\ \vdots & \vdots & \ddots & \vdots \\ h_{L-1} & h_L & \cdots & 0 \\ h_L & 0 & \cdots & 0 \end{pmatrix}, \quad (15)$$

where $\mathscr{H}(\cdot)$ is an operator that builds a Hankel matrix from its vector argument as shown above and the channel coefficient vector is defined as

$$\mathbf{h} = [h_0 \dots h_L]^{\mathsf{T}} \in \mathbb{C}^{(L+1)}. \quad (16)$$

In the next section, we establish a link between the Parafac decomposition (14) and the simultaneous matrix diagonalization approach. Then, we present a SS LS algorithm to blindly estimate the channel coefficient vector.

4. Blind SISO channel identification using the Parafac decomposition of the 4th-order output cumulant tensor

Slicing the cumulant tensor $\mathscr{C}^{(3,y)}$ along each of its three dimensions yields $2L+1$ cumulant matrices $\mathbf{C}_{i..}$, $\mathbf{C}_{.j.}$ and $\mathbf{C}_{..k}$, $i,j,k \in [1, 2L+1]$, respectively, each of which being of dimensions $(2L+1)\times(2L+1)$. In Fig. 1b we show the frontal slices $\mathbf{C}_{..k}$, obtained by fixing the third index k, which are given by

$$\begin{aligned}\mathbf{C}_{..k} &= \sum_{i=1}^{2L+1}\sum_{j=1}^{2L+1} c_{ijk}\mathbf{e}_i^{(2L+1)}\mathbf{e}_j^{(2L+1)^{\mathsf{T}}} \\ &= \gamma_{4,s}\sum_{l=0}^{L} h_l^* h_{l+k-L-1}\mathbf{H}_{.l}\mathbf{H}_{.l}^{\mathsf{H}} \\ &= \gamma_{4,s}\mathbf{H}D_k(\mathbf{\Sigma})\mathbf{H}^{\mathsf{H}}, \end{aligned} \quad (17)$$

for $k \in [1, 2L+1]$, where

$$\mathbf{\Sigma} = \mathbf{H}\,\mathrm{Diag}(\mathbf{h})^* \in \mathbb{C}^{(2L+1)\times(L+1)}. \quad (18)$$

Notice that the frontal slices defined in (17) have the form of $\mathbf{T}_{..k}$ in Table 2 with the three loading factors depending on $\mathbf{H}$ as follows:

$$\mathbf{A}^{(1)} = \mathbf{H}, \quad \mathbf{A}^{(2)} = \mathbf{H}^* \quad \text{and} \quad \mathbf{A}^{(3)} = \gamma_{4,s}\mathbf{\Sigma}. \quad (19)$$

Hence, by analogy with the other equations in Table 2, we get the following expressions of the vertical and horizontal slices:

$$\mathbf{C}_{.j.} = \gamma_{4,s}\mathbf{\Sigma}D_j(\mathbf{H})^*\mathbf{H}^{\mathsf{T}}, \quad j \in [1, 2L+1], \quad (20)$$

$$\mathbf{C}_{i..} = \gamma_{4,s}\mathbf{H}^* D_i(\mathbf{H})\mathbf{\Sigma}^{\mathsf{T}}, \quad i \in [1, 2L+1]. \quad (21)$$

It is interesting to note that Eqs. (17), (20) and (21) suggest that the Parafac components of the cumulant tensor can be obtained from the factorization of a 2D slice or, more precisely, from the simultaneous diagonalization of a set of matrices, such as $\mathbf{C}_{..k}$, $k \in [1, 2L+1]$. However, since the channel matrix $\mathbf{H}$ is not unitary, it cannot be recovered from a simple application of a diagonalization technique, such as SVD,[3] without a previous orthonormalization of the slices $\mathbf{C}_{..k}$. This extra operation, often referred to as *pre-whitening*, consists in constructing a new set of *modified* cumulant matrices that admit an orthogonal decomposition. The modified cumulant matrices are obtained by means of a linear transformation $\mathbf{W}$ so that $\bar{\mathbf{C}}_{..k} = \mathbf{W}\mathbf{C}_{..k}\mathbf{W}^{\mathsf{H}}$, with $\mathbf{WH}$ unitary. The computation of matrix $\mathbf{W}$ usually requires resorting to SOS. This additional step, very common in HOS-based methods [10,44,45], is time-consuming and often responsible for increased estimation errors [30,31]. Without resorting to a tensor formalism, the joint-diagonalization approach is exploited in [11], using cumulant matrices that can be obtained from (17), with non-negative time-lags only, i.e. $0 \leqslant \tau_1, \tau_2, \tau_3 \leqslant L$ or, equivalently:

$$L+1 \leqslant i,j,k \leqslant 2L+1.$$

Eq. (14) shows that the rank of tensor $\mathscr{C}^{(3,y)}$ equals the number F of non-zero coefficients in $\mathbf{h}$, so that $F \leqslant L+1$. Assumption A4 ensures that $F \geqslant 2$. Due to its Hankel structure, $\mathbf{H}$ is full column-rank and then $k_{A^{(1)}} = k_{A^{(2)}} = r_H = L+1$. From (18) and assumption A4, we deduce that $r_\Sigma = F \geqslant 2$. If all the channel coefficients are nonzero, then $F = L+1$ and we have $k_{A^{(3)}} = r_{\mathbf{\Sigma}} = L+1$; otherwise $k_{A^{(3)}} = 0$ because, if $F < L+1$, at least one column of $\mathbf{\Sigma}$ is zero. From the Kruskal uniqueness condition (4), we conclude that, if $F = L+1$, then $k_{A^{(1)}} + k_{A^{(2)}} + k_{A^{(3)}} = 3L+3 \geqslant 2F+2$; otherwise, if $F < L+1$, then $k_{A^{(1)}} + k_{A^{(2)}} + k_{A^{(3)}} = 2L+2 \geqslant$

[3] It is well known that the SVD of a matrix yields a factorization of the type $\mathbf{X} = \mathbf{U}\mathbf{D}\mathbf{V}^{\mathsf{H}}$, with $\mathbf{D}$ diagonal and $\mathbf{U}$ and $\mathbf{V}$ unitary. When dealing with Hermitian matrices, this orthogonality constraint also applies to EVD.

Table 3
Parafac formulae for the 3rd-order tensor $\mathscr{C}^{(3,y)}$

Direction	Tensor 2D slices	Unfolded representations
Horizontal	$\mathbf{C}_{i\cdot\cdot} = \gamma_{4,s}\mathbf{H}^* D_i(\mathbf{H})\mathbf{\Sigma}^{\mathsf{T}}$	$\mathbf{C}_{[1]} = \gamma_{4,s}(\mathbf{H} \diamond \mathbf{H}^*)\mathbf{\Sigma}^{\mathsf{T}}$
Vertical	$\mathbf{C}_{\cdot j\cdot} = \gamma_{4,s}\mathbf{\Sigma} D_j(\mathbf{H}^*)\mathbf{H}^{\mathsf{T}}$	$\mathbf{C}_{[2]} = \gamma_{4,s}(\mathbf{H}^* \diamond \mathbf{\Sigma})\mathbf{H}^{\mathsf{T}}$
Frontal	$\mathbf{C}_{\cdot\cdot k} = \gamma_{4,s}\mathbf{H} D_k(\mathbf{\Sigma})\mathbf{H}^{\mathsf{H}}$	$\mathbf{C}_{[3]} = \gamma_{4,s}(\mathbf{\Sigma} \diamond \mathbf{H})\mathbf{H}^{\mathsf{H}}$

$2F+2$, which implies that the Kruskal condition is always satisfied. Thus, any set $\{\bar{\mathbf{A}}^{(1)}, \bar{\mathbf{A}}^{(2)}, \bar{\mathbf{A}}^{(3)}\}$ satisfying the Parafac decomposition of the cumulant tensor $\mathscr{C}^{(3,y)}$ has the form (3), with $\mathbf{A}^{(1)}$, $\mathbf{A}^{(2)}$ and $\mathbf{A}^{(3)}$ given in (19).

Tensor $\mathscr{C}^{(3,y)}$ can be expressed under unfolded matrix representations obtained by stacking up the 2D slices (17), (20) or (21). Taking the equations in Table 2 into account and using the correspondences (19), we obtain the equations in Table 3. These unfolded matrices can be used to estimate $\mathbf{H}$ and $\mathbf{\Sigma}$ by means of the TALS algorithm. Once $\mathbf{H}$ is estimated it is straightforward to deduce the channel parameters. However, we can improve the efficiency of the estimation procedure by coupling both estimation steps, i.e. taking the relationships between the channel coefficient vector $\mathbf{h}$ and the matrices $\mathbf{H}$ and $\mathbf{\Sigma}$ into account, thus eliminating column scaling and permutation ambiguities [46,47].

SS-LS Parafac-based blind channel identification algorithm

In this section, we propose a SS-LS algorithm to estimate the channel coefficient vector $\mathbf{h}$ by means of the previously described tensor decomposition. Using (18), we can express $\mathbf{C}_{[1]}$ (given in Table 3) as follows:

$$\mathbf{C}_{[1]} = \gamma_{4,s}(\mathbf{H} \diamond \mathbf{H}^*)\mathrm{Diag}(\mathbf{h})^*\mathbf{H}^{\mathsf{T}}. \tag{22}$$

Applying property (P-1) to this equation, we get

$$\mathrm{vec}(\mathbf{C}_{[1]}) = \gamma_{4,s}(\mathbf{H} \diamond \mathbf{H} \diamond \mathbf{H}^*)\mathbf{h}^*. \tag{23}$$

The channel coefficient vector $\mathbf{h}$ can be obtained by iteratively minimizing the following LS cost function:

$$\psi(\mathbf{h}^*, \hat{\mathbf{h}}^{(r-1)}) \triangleq \|\mathrm{vec}(\mathbf{C}_{[1]}) - \gamma_{4,s}\hat{\mathbf{G}}^{(r-1)}\mathbf{h}^*\|^2, \tag{24}$$

where

$$\hat{\mathbf{G}}^{(r-1)} = \hat{\mathbf{H}}^{(r-1)} \diamond \hat{\mathbf{H}}^{(r-1)} \diamond \hat{\mathbf{H}}^{(r-1)*} \tag{25}$$

and, from (15), $\hat{\mathbf{H}}^{(r-1)} = \mathscr{H}(\hat{\mathbf{h}}^{(r-1)})$. At iteration r, we get $\hat{\mathbf{h}}^{(r)} = \arg\min \psi(\mathbf{h}^*, \hat{\mathbf{h}}^{(r-1)})$. The algorithm is initialized with a Hankel matrix $\hat{\mathbf{H}}^{(0)}$ in which the first column is $[\mathbf{0}_{(L)}^{\mathsf{T}}\ \hat{\mathbf{h}}^{(0)\mathsf{T}}]^{\mathsf{T}}$ and the last row is $[\hat{h}_L^{(0)}\ \mathbf{0}_{(L)}^{\mathsf{T}}]$, where $\hat{\mathbf{h}}^{(0)} = [1\ \mathbf{v}^{\mathsf{T}}]^{\mathsf{T}}$, $\mathbf{v} \in \mathbb{C}^{(L)}$ is a Gaussian random vector and $\mathbf{0}_{(L)}$ is an all-zeros vector of dimension L. The algorithm is iterated until $\|\hat{\mathbf{h}}^{(r)} - \hat{\mathbf{h}}^{(r-1)}\|/\|\hat{\mathbf{h}}^{(r)}\| \leqslant \varepsilon$, where ε is an arbitrary small positive constant. In order to take the constraint $h_0 = 1$ into account at each iteration r, we normalize the previous estimate $\hat{\mathbf{h}}^{(r-1)}$ with respect to its first entry $\hat{h}_0^{(r-1)}$ before using it to update $\hat{\mathbf{H}}^{(r-1)}$ using (15). Then, $\hat{\mathbf{G}}^{(r-1)}$ is updated from (25) using $\hat{\mathbf{H}}^{(r-1)}$. The normalization step eliminates the scaling ambiguity and forcing the Hankel structure allows us to avoid column permutation in the Parafac decomposition.

The above described strategy ensures the Hankel structure of $\mathbf{H}$ at each iteration, taking advantage of its full-rank property to make the tensor decomposition essentially unique and the channel estimation free from ambiguities. Furthermore, a SS-LS minimization procedure is used instead of the classical trilinear ALS algorithm. For that reason, our method should be expected to increase the convergence speed. After initializing $\hat{\mathbf{h}}^{(0)}$ as a Gaussian random vector, the SS-LS Parafac-based Blind Channel Identification (SS-LS PBCI) algorithm can be summarized as follows, for $r \geqslant 1$:

1. Use (15) to build $\hat{\mathbf{H}}^{(r-1)} = \mathscr{H}(1/\hat{h}_0^{(r-1)}\hat{\mathbf{h}}^{(r-1)})$.
2. Compute $\hat{\mathbf{G}}^{(r-1)}$ using (25).
3. Minimize the cost function (24) so that

$$\hat{\mathbf{h}}^{(r)*} = \gamma_{4,s}^{-1}\hat{\mathbf{G}}^{(r-1)\#}\mathrm{vec}(\mathbf{C}_{[1]}). \tag{26}$$

4. Iterate until $\|\hat{\mathbf{h}}^{(r)} - \hat{\mathbf{h}}^{(r-1)}\|/\|\hat{\mathbf{h}}^{(r)}\| \leqslant \varepsilon$.

The identifiability of the channel coefficient vector $\mathbf{h}$ depends on the rank of the matrix $\hat{\mathbf{G}}^{(r-1)} \in \mathbb{C}^{(2L+1)^3 \times (L+1)}$. Due to its Hankel structure, given by (15), $\hat{\mathbf{H}}^{(r-1)}$ is ensured to be full column-rank. So, we have $k_{\hat{\mathbf{H}}^{(r-1)}} = L+1$ and therefore $\hat{\mathbf{G}}^{(r-1)}$, defined in (25) as a double Khatri–Rao product, is also full column-rank [48], which implies the uniqueness of the LS solution given by (26).

5. MIMO channel model and 4th-order spatial cumulant tensors

Let us consider an instantaneous MIMO channel with Q signal sources and M receive antennas. The

signals received at the front-end of the antenna array at the time-instant n, are modeled as a complex-valued vector $\mathbf{y}(n) \in \mathbb{C}^M$ written as

$$\mathbf{y}(n) = \mathbf{H}\mathbf{s}(n) + \boldsymbol{\upsilon}(n), \tag{27}$$

where the elements of the instantaneous mixing matrix $\mathbf{H} \in \mathbb{C}^{M\times Q}$ are the MIMO channel coefficients h_{mq}. The following assumptions are made:

B1. The source signals $s_q(n)$ are stationary, ergodic and mutually independent with symmetric distribution, zero-mean and non-zero kurtosis $\gamma_{4,s_q} = c_{4,s_q}(0,0,0)$ assumed to be known.
B2. The vector $\boldsymbol{\upsilon}(n) \in \mathbb{C}^{M\times 1}$ is the additive Gaussian noise at the output of the antenna array. It is independent from the source signals and has an unknown spatial correlation.
B3. The MIMO channel matrix $\mathbf{H} \in \mathbb{C}^{M\times Q}$ has elements $h_{m,q}$, representing a Rayleigh flat fading propagation environment, i.e. the channel coefficients are complex constants with real and imaginary parts driven from a continuous Gaussian distribution.

Assuming that γ_{4,s_q} is known is not really constraining in the context of telecommunication systems, where the source modulation schemes are generally known at the receiver. Although usual, this assumption is not absolutely necessary and could be relaxed. Note also that we do not constrain the source kurtoses to have equal sign. Assumption B3 allows us to say that $\mathbf{H}$ is full k-rank with probability one, even when $M < Q$.

We now consider the blind MIMO channel identification problem using 4th-order output statistics only. It is well known that solutions to this problem only exist up to a column scaling and permutation indeterminacy. The 4th-order spatial cumulants of the array outputs are defined as

$$C_{4,y}(i,j,k,l) \triangleq \mathrm{cum}[y_i^*(n), y_j(n), y_k^*(n), y_l(n)]. \tag{28}$$

Under the above mentioned assumptions, it is straightforward to show that

$$C_{4,y}(i,j,k,l) = \sum_{q=1}^{Q} \gamma_{4,s_q} h_{iq}^* h_{jq} h_{kq}^* h_{lq}, \tag{29}$$

Notice that the cumulants $C_{4,y}(i,j,k,l)$ only exist for $1 \leqslant i,j,k,l \leqslant M$. Let us define the 4th-order tensor $\mathscr{C}^{(4,y)} \in \mathbb{C}^{M\times M\times M\times M}$, in which the element in position (i,j,k,l) corresponds to $C_{4,y}(i,j,k,l)$, so that

$$\mathscr{C}^{(4,y)} = \sum_{i=1}^{M}\sum_{j=1}^{M}\sum_{k=1}^{M}\sum_{l=1}^{M} C_{4,y}(i,j,k,l)\mathbf{e}_i^{(M)} \circ \mathbf{e}_j^{(M)} \circ \mathbf{e}_k^{(M)} \circ \mathbf{e}_l^{(M)}. \tag{30}$$

Replacing (29) into (30) we can rewrite $\mathscr{C}^{(4,y)}$ as a sum of Q rank-1 tensors, each one being written as an outer product involving four vectors:

$$\mathscr{C}^{(4,y)} = \sum_{q=1}^{Q} \mathbf{H}_{\cdot q}^* \circ \mathbf{H}_{\cdot q} \circ \mathbf{H}_{\cdot q}^* \circ (\gamma_{4,s_q}\mathbf{H}_{\cdot q}), \tag{31}$$

where $\mathbf{H}_{\cdot q} = \sum_{m=1}^{M} h_{m,q}\mathbf{e}_m^{(M)}$, $q \in [1, Q]$. Eq. (31) is the Parafac decomposition of tensor $\mathscr{C}^{(4,y)}$, where the four loading factors depend on $\mathbf{H}$, as follows:

$$\mathbf{A}^{(1)} = \mathbf{H}^*, \quad \mathbf{A}^{(2)} = \mathbf{H}, \quad \mathbf{A}^{(3)} = \mathbf{H}^*$$

and

$$\mathbf{A}^{(4)} = \mathbf{H}\boldsymbol{\Gamma}_{4,s}, \tag{32}$$

where

$$\boldsymbol{\Gamma}_{4,s} = \mathrm{Diag}(\gamma_{4,s_1}, \ldots, \gamma_{4,s_Q}). \tag{33}$$

Using the above correspondences, the 2D representations of $\mathscr{C}^{(4,y)}$ can be deduced from the equations in Table 1. For instance, slicing $\mathscr{C}^{(4,y)}$ along the $k \times l$ plane gives the following matrix $\mathbf{C}_{[1,2]} \in \mathbb{C}^{M^3\times M}$:

$$\mathbf{C}_{[1,2]} = (\mathbf{H}^* \diamond \mathbf{H} \diamond \mathbf{H}^*)\boldsymbol{\Gamma}_{4,s}\mathbf{H}^{\mathsf{T}}. \tag{34}$$

According to the unfolding procedure described in Section 2, $\mathbf{C}_{[1,2]}$ is obtained[4] by stacking matrices $\mathbf{C}_{[2]_i}$, $i \in [1, M]$, defined as $\mathbf{C}_{[2]_i} = [\mathbf{C}_{i1\cdot\cdot}^{\mathsf{T}}, \ldots, \mathbf{C}_{iM\cdot\cdot}^{\mathsf{T}}]^{\mathsf{T}}$, where $\mathbf{C}_{ij\cdot\cdot}$ are the 2D slices of tensor $\mathscr{C}^{(4,y)}$ along the $k \times l$ plane, with $[\mathbf{C}_{ij\cdot\cdot}]_{kl} = C_{4,y}(i,j,k,l)$, $k,l \in [1, M]$.

From the general equations given in Table 1, we easily get $\mathbf{C}_{ij\cdot\cdot} = \mathbf{H}^* D_i(\mathbf{H}^*)\boldsymbol{\Gamma}_{4,s} D_j(\mathbf{H})\mathbf{H}^{\mathsf{T}}$. This formulation naturally leads to a simultaneous diagonalization problem. A similar set of equations can be obtained from the output quadricovariance matrix, which is the basic idea behind the FOBIUM algorithm [49]. In fact, FOBIUM can be viewed as a 4th-order extension of the classic SOS-based SOBI algorithm [10]. Indeed, it needs a 4th-order prewhitening step and requires non-Gaussian sources having kurtoses with the same sign and different

[4] In practice, the lth-column of $\mathbf{C}_{[1,2]}$ is formed with the elements $C_{4,y}(i,j,k,l)$ arranged in such a way that the indices $i,j,k \in [1, M]$ vary in nested loops with k being the innermost one (fastest) and i the outermost one (slowest).

trispectra. By exploiting the Kronecker structure of a particular unfolded tensor representation, the method reported in [32] solves the canonical tensor decomposition problem by means of a simultaneous matrix diagonalization. Making use of similar ideas, the algorithms proposed in [14] have the advantage of permitting weaker uniqueness conditions and hence, theoretically allowing for the identification of more sources for a fixed number of antennas. Although avoiding pre-whitening, these latter algorithms still have to solve two optimization problems in order to extract MIMO parameters from an initial EVD-based estimate. On the contrary, we propose solutions that can be obtained from a single minimization problem, under very mild assumptions.

5.1. Uniqueness

Notice from (31) that the rank of the 4th-order tensor $\mathscr{C}^{(4,y)}$ is $F=Q$. In addition, since $\mathbf{H}$ is assumed to be full k-rank, we have $k_{A^{(1)}}=k_{A^{(2)}}=k_{A^{(3)}}=k_{A^{(4)}}=r_H=\min(M,Q)$. We conclude from (4) that the Kruskal uniqueness condition reduces to

$$4r_H \geqslant 2Q+3. \tag{35}$$

The two following cases can be considered:

- The MIMO channel is an overdetermined system, i.e. $M \geqslant Q$. In this case $r_H=Q$ and (35) states that the Parafac decomposition of $\mathscr{C}^{(4,y)}$ is essentially unique if $Q \geqslant 3/2$, i.e. $Q>1$. There are no further constraints on the number of sensors.
- The MIMO channel is an underdetermined system, i.e. $M<Q$. In this case $r_H=M$ and hence equation (35) becomes

$$Q \leqslant 2M-2. \tag{36}$$

Table 4 gives the maximum number of users that our model can deal with, for a given number of receiving antennas varying from $M=2$ to 7. Under these conditions, the Parafac decomposition of tensor $\mathscr{C}^{(4,y)}$ is unique, up to trivial permutation and scaling ambiguities. In other words, the loading factors of $\mathscr{C}^{(4,y)}$ are given by (3) with $\mathbf{A}^{(1)}$, $\mathbf{A}^{(2)}$, $\mathbf{A}^{(3)}$ and $\mathbf{A}^{(4)}$ defined in (32).

Table 4
Relationship between M and Q for the uniqueness of $\mathscr{C}^{(4,y)}$

Number of antennas	$M=$	2	3	4	5	6	7
Maximum number of sources	$Q\leqslant$	2	4	6	8	10	12

5.2. Reduced-order cumulant tensor

It is possible to reduce the 4th-order tensor defined in (30) to a 3rd-order one by combining its 3D slices, thus reducing the complexity of the above described tensor decomposition. Without loss of generality, we freeze the index k in the cumulant definition (28), and define the 3D slices as

$$\mathscr{C}_k^{(3,y)} = \sum_{i=1}^{M}\sum_{j=1}^{M}\sum_{l=1}^{M} C_{4,y}(i,j,k,l)\mathbf{e}_i^{(M)}\circ\mathbf{e}_j^{(M)}\circ\mathbf{e}_l^{(M)} \tag{37}$$

$$= \sum_{q=1}^{Q}\gamma_{4,s_q}h_{kq}^{*}\mathbf{H}_{\cdot q}^{*}\circ\mathbf{H}_{\cdot q}\circ\mathbf{H}_{\cdot q}. \tag{38}$$

Summing these slices for all $k\in[1,M]$ we get

$$\mathscr{C}^{(3,y)} = \sum_{k=1}^{M}\mathscr{C}_k^{(3,y)} = \sum_{q=1}^{Q}\mathbf{H}_{\cdot q}^{*}\circ\mathbf{H}_{\cdot q}\circ\left(\gamma_{4,s_q}\mathbf{H}_{\cdot q}\sum_{k=1}^{M}h_{kq}^{*}\right). \tag{39}$$

From this equation, we conclude that $\mathscr{C}^{(3,y)}$ is a 3rd-order Parafac model with the following loading factors:

$$\mathbf{A}^{(1)}=\mathbf{H}^{*},\ \mathbf{A}^{(2)}=\mathbf{H} \quad\text{and}\quad \mathbf{A}^{(3)}=\mathbf{H}\boldsymbol{\Delta}\boldsymbol{\Gamma}_{4,s}, \tag{40}$$

where $\boldsymbol{\Delta}$ is a diagonal matrix given by

$$\boldsymbol{\Delta}=\sum_{k=1}^{M}D_k(\mathbf{H})^{*}. \tag{41}$$

Using the correspondences (40) in the equations of Table 2, we get the unfolded representations of tensor $\mathscr{C}^{(3,y)}$. Selecting, for instance, the horizontal slicing direction (first row in Table 2), we have

$$\mathbf{C}_{[1]}=(\mathbf{H}^{*}\diamond\mathbf{H})\boldsymbol{\Gamma}_{4,s}\boldsymbol{\Delta}\mathbf{H}^{\mathsf{T}}. \tag{42}$$

In practice, $\mathbf{C}_{[1]}$ is obtained by stacking the matrices $\mathbf{C}_{i\cdot\cdot}$, $i\in[1,M]$, where $[\mathbf{C}_{i\cdot\cdot}]_{jl}=\sum_k C_{4,y}(i,j,k,l)$, $j,l\in[1,M]$. This is equivalent to $[\mathbf{C}_{[1]}]_{(i-1)M+j,l}=\sum_k C_{4,y}(i,j,k,l)$, $i,j,l\in[1,M]$.

Due to assumption B3, the diagonal entries of $\boldsymbol{\Delta}$ are nonzero with probability one. This allows us to conclude that $k_{A^{(1)}}=k_{A^{(2)}}=k_{A^{(3)}}=r_H=\min(M,Q)$ and the Kruskal uniqueness condition (4) becomes $3r_H\geqslant 2Q+2$. This yields $Q\geqslant 2$ for $M\geqslant Q$ and $Q\leqslant(3M-2)/2$ when $M<Q$. Table 5 shows the maximum number of sources for a given number of receive antennas varying from $M=2$ to 7 so that

Table 5
Relationship between M and Q for the uniqueness of the Parafac decomposition of $\mathscr{C}^{(3,y)}$

Number of antennas	$M=$	2	3	4	5	6	7
Maximum number of sources	$Q\leqslant$	2	3	5	6	8	9

the model is unique. Under these conditions, the Parafac loading factors of $\mathscr{C}^{(3,y)}$ can be written as in (3) with $\mathbf{A}^{(1)}$, $\mathbf{A}^{(2)}$ and $\mathbf{A}^{(3)}$ defined in (40).

6. Parafac-based blind MIMO channel identification (PBMCI) algorithms

Based on the explicit relationships presented in the previous section, we now propose two algorithms to estimate the instantaneous MIMO mixing matrix, up to column scaling and permutation. This is achieved by means of a single (non-alternating) LS minimization procedure, thanks to the symmetry properties of the 4th-order cumulant. The basic idea behind the algorithms proposed in the sequel is to consider only one of the unfolded representations of the cumulant tensor $\mathscr{C}^{(4,y)}$ by exploiting the relationships (32) (or (40) in the case of $\mathscr{C}^{(3,y)}$). This is equivalent to rewrite any of the unfolded tensor representations defined in Table 1 (resp. Table 2) in terms of $\mathbf{A}^{(p)}$, for a fixed p. After that, we also present the procedures for estimating the mixing matrix using the classical ALS-type algorithms described in Section 2.

6.1. 4D SS-LS PBMCI algorithm

Eq. (34) enables us to estimate the MIMO channel matrix by iteratively minimizing a single LS cost function, written as follows:

$$\psi(\hat{\mathbf{H}}_{r-1},\mathbf{H})\triangleq\|\mathbf{C}_{[1,2]}-(\hat{\mathbf{H}}_{r-1}^{*}\diamond\hat{\mathbf{H}}_{r-1}\diamond\hat{\mathbf{H}}_{r-1}^{*})\boldsymbol{\Gamma}_{4,s}\mathbf{H}^{\mathsf{T}}\|_{\mathrm{F}}^{2}, \tag{43}$$

where r denotes the iteration number. The iterative minimization of $\psi(\hat{\mathbf{H}}_{r-1},\mathbf{H})$ yields the following LS solution:

$$\begin{aligned}\hat{\mathbf{H}}_{r}^{\mathsf{T}}&\triangleq\arg\min_{\mathbf{H}}\psi(\hat{\mathbf{H}}_{r-1},\mathbf{H})\\&=\boldsymbol{\Gamma}_{4,s}^{-1}(\hat{\mathbf{H}}_{r-1}^{*}\diamond\hat{\mathbf{H}}_{r-1}\diamond\hat{\mathbf{H}}_{r-1}^{*})^{\#}\mathbf{C}_{[1,2]},\end{aligned} \tag{44}$$

where $\hat{\mathbf{H}}_0$ is initialized as a complex $M\times Q$ Gaussian random matrix. In order to improve estimation at each iteration $r\geqslant 1$, before computing $\hat{\mathbf{H}}_r$, we normalize each column of the previous estimate $\hat{\mathbf{H}}_{r-1}$ by dividing it by its 2-norm. The algorithm is stopped when $\|\hat{\mathbf{H}}_r-\hat{\mathbf{H}}_{r-1}\|_{\mathrm{F}}/\|\hat{\mathbf{H}}_r\|_{\mathrm{F}}\leqslant\varepsilon$, where ε is an arbitrary small positive constant.

In the underdetermined case, the uniqueness of the Parafac decomposition of $\mathscr{C}^{(4,y)}$ is ensured under the condition stated by the Kruskal Theorem (4), which leads to the relationships between M and Q given in Table 4. Due to the lemma introduced in [48], if $k_{H^*}+k_H\geqslant Q+1$ then $\mathbf{H}^*\diamond\mathbf{H}$ is full column-rank, which yields $k_{H^*\diamond H}=Q$. In the underdetermined case, we have $k_H=M$ and hence the previous condition becomes $Q\leqslant 2M-1$. Applying the same lemma on the double Khatri–Rao product $\mathbf{H}^*\diamond\mathbf{H}\diamond\mathbf{H}^*$, the condition $k_{H^*\diamond H}+k_H^*\geqslant Q+1$ is equivalent to $Q+M\geqslant Q+1$, which is always satisfied, implying that the double Khatri–Rao product is full column rank, which guarantees the uniqueness of the LS solution given by (44). Notice that this constraint is slightly weaker than the uniqueness condition (36), so that, by satisfying this latter one, we can ensure that any matrix $\bar{\mathbf{H}}$ obeying to (34) is such that $\bar{\mathbf{H}}=\mathbf{H}\boldsymbol{\Lambda}\boldsymbol{\Pi}$, where $\boldsymbol{\Pi}$ is a permutation matrix and $\boldsymbol{\Lambda}$ a diagonal matrix with unit-modulus diagonal elements. Therefore, since we are dealing with complex values, the scaling ambiguity is not completely eliminated but it is reduced to a single phase indeterminacy. The above described method will be referred to as the 4D SS-LS Parafac-based Blind MIMO Channel Identification (4D SS-LS PBMCI) algorithm. The above developments were presented, without loss of generality, for $\mathbf{C}_{[1,2]}$. Any other equation in Table 1 can be used instead.

6.2. 3D SS-LS PBMCI algorithm

The SS approach can also be formulated using tensor $\mathscr{C}^{(3,y)}$ defined in (39). Eq. (42) yields the following LS cost function:

$$\psi(\hat{\mathbf{H}}_{r-1},\mathbf{H})\triangleq\|\mathbf{C}_{[1]}-(\hat{\mathbf{H}}_{r-1}^{*}\diamond\hat{\mathbf{H}}_{r-1})\boldsymbol{\Gamma}_{4,s}\hat{\boldsymbol{\Delta}}_{r-1}\mathbf{H}^{\mathsf{T}}\|_{\mathrm{F}}^{2}, \tag{45}$$

where $\hat{\boldsymbol{\Delta}}_{r-1}=\sum_k D_k(\hat{\mathbf{H}}_{r-1}^{*})$. Iteratively minimizing (45) leads to

$$\hat{\mathbf{H}}_{r}^{\mathsf{T}}=\boldsymbol{\Gamma}_{4,s}^{-1}\hat{\boldsymbol{\Delta}}_{r-1}^{-1}(\hat{\mathbf{H}}_{r-1}^{*}\diamond\hat{\mathbf{H}}_{r-1})^{\#}\mathbf{C}_{[1]}. \tag{46}$$

Here again, $\hat{\mathbf{H}}_0$ is initialized as a complex $M\times Q$ Gaussian random matrix and $\hat{\mathbf{H}}_{r-1}$ is normalized before computing the next estimate $\hat{\mathbf{H}}_r$. This method will be called the 3D SS-LS PBMCI algorithm. Sufficient uniqueness conditions are given

in Table 5. According to the lemma introduced in [38], we need $Q \leqslant 2M-1$ in order to ensure that the Khatri–Rao product in (46) is full column-rank, which guarantees the uniqueness of the LS solution. This condition is weaker than the uniqueness conditions discussed in Section 5.2.

6.3. ALS-type PBMCI algorithms

Classical ALS-type algorithms can also be used to solve the blind channel identification problem. In particular, the QALS and TALS algorithms described in Section 2 provide solutions to the Parafac decomposition of tensors $\mathscr{C}^{(4,y)}$ and $\mathscr{C}^{(3,y)}$, using the equations provided in Tables 1 and 2, respectively. Although these algorithms do not take the relationships between the loading factors into account, we can nevertheless initialize QALS with a complex $M \times Q$ Gaussian random matrix $\hat{\mathbf{A}}_0^{(2)}$ and then deduce $\hat{\mathbf{A}}_0^{(3)}$ and $\hat{\mathbf{A}}_0^{(4)}$ using (32). After that, the QALS algorithm is started with the computation of $\hat{\mathbf{A}}_1^{(1)}$ using (7).

Denoting by $r=\infty$ the iteration at which convergence is reached, the estimated loading factors $\hat{\mathbf{A}}_\infty^{(p)}$, $p=1,\ldots,4$, have the form (3). Taking the correspondences (32) into account, this yields the following different equations for estimating $\mathbf{H}$, up to column scaling and permutation:

$$\hat{\mathbf{A}}_\infty^{(1)} = \hat{\mathbf{H}}^{(1)*}\boldsymbol{\Lambda}_1\boldsymbol{\Pi},$$

$$\hat{\mathbf{A}}_\infty^{(2)} = \hat{\mathbf{H}}^{(2)}\boldsymbol{\Lambda}_2\boldsymbol{\Pi},$$

$$\hat{\mathbf{A}}_\infty^{(3)} = \hat{\mathbf{H}}^{(3)*}\boldsymbol{\Lambda}_3\boldsymbol{\Pi},$$

$$\hat{\mathbf{A}}_\infty^{(4)} = \hat{\mathbf{H}}^{(4)}\boldsymbol{\Gamma}_{4,s}\boldsymbol{\Lambda}_4\boldsymbol{\Pi}. \tag{47}$$

The estimates $\hat{\mathbf{H}}^{(1)}$ and $\hat{\mathbf{H}}^{(3)}$ can be obtained by simple conjugation of $\hat{\mathbf{A}}_\infty^{(1)}$ and $\hat{\mathbf{A}}_\infty^{(3)}$, respectively. The above procedure will be referred to as the quadrilinear ALS Parafac-based blind MIMO channel identification (QALS-PBMCI) algorithm.

Concerning the TALS algorithm, it can also be initialized with a complex $M \times Q$ Gaussian random matrix $\hat{\mathbf{A}}_0^{(2)}$ and $\hat{\mathbf{A}}_0^{(3)}$ is deduced from (40) and (41). The correspondences (40) indicate that the loading factors $\hat{\mathbf{A}}_\infty^{(1)*}$, $\hat{\mathbf{A}}_\infty^{(2)}$ and $\hat{\mathbf{A}}_\infty^{(3)}$ are estimates of $\mathbf{H}$, up to column permutation and scaling. This method will be called the trilinear ALS Parafac-based blind MIMO channel identification (TALS-PBMCI) algorithm.

Although scaling and permutation ambiguities are not explicitly solved, these indeterminacies do not represent a concern in the context of blind mixture identification and, in the overdetermined case, it is even possible to recover the source signals.

7. Computer simulations

In this section, we present some computer simulation results in order to assess the performance of the proposed blind identification algorithms. We first consider a SISO-FIR communication channel and compare the performance of the SS-LS PBCI method with the results obtained using the well-known FOSI algorithm, which is based on a joint diagonalization technique. As suggested by the authors of [11], the FOSI algorithm performance is evaluated by averaging the results of the two solutions proposed therein. We also compare our method with the optimal algebraic solution in the total least squares (TLS) sense, proposed in [5].

Afterwards, we consider a *quasi-static* MIMO channel scenario where the complex channel coefficients are drawn from a Rayleigh distribution and are assumed to be time-invariant within the duration of a time-slot, composed of N symbol periods. The performance of the QALS-PBMCI and TALS-PBMCI algorithms are compared with those of the SS-LS PBMCI algorithms. Although our main interest is in mixture identification, we also provide results concerning the recovery of the transmitted symbols using the channel estimates obtained with the proposed identification methods in both SISO and MIMO cases.

7.1. SISO channel identification

The parametric channel estimation performance is evaluated by means of the normalized mean squared error (NMSE) of the estimator, computed by means of the following formula:

$$\mathtt{NMSE} = \frac{1}{P}\sum_{p=1}^{P}\frac{\|\hat{\mathbf{h}}_{\langle p\rangle}^{(\infty)} - \mathbf{h}\|^2}{\|\mathbf{h}\|^2}, \tag{48}$$

where P is the number of Monte Carlo simulations and $\hat{\mathbf{h}}_{\langle p\rangle}^{(\infty)}$ is the channel estimate obtained after convergence of the experiment $p \in [1,P]$, assuming perfect knowledge of the channel memory L. Except otherwise stated, 4th-order cumulants were estimated using $N=1000$ output data samples. For each Monte Carlo simulation, a different complex channel coefficient vector was randomly generated in such a way that minimum-phase,

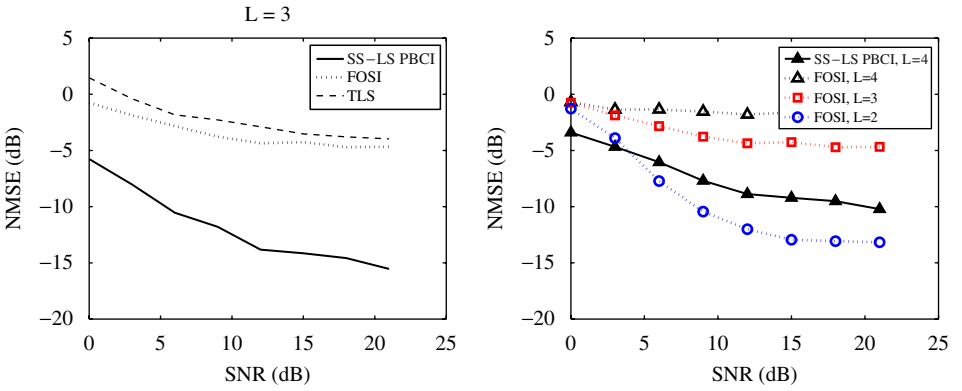

Fig. 2. NMSE performance with QPSK modulation.

nonminimum-phase as well as maximum-phase channels may occur. Furthermore, we allow for some channels to be possibly ill-conditioned (h_L very small in magnitude). The results illustrated in the following curves represent the average of $P = 200$ Monte Carlo runs. The input signal is QPSK modulated.

In Fig. 2, the NMSE is plotted against the signal-to-noise ratio (SNR) for SS-LS PBCI, FOSI and TLS algorithms. The curves on the left-hand side show that our approach performs better than both, the FOSI algorithm and the TLS solution, for channels with memory $L = 3$. The relative behavior of the algorithms shown in that figure was also verified for $L = 2$ and 4. On the right-hand side of Fig. 2, we compare the results of SS-LS PBCI for $L = 4$ with those of the FOSI algorithm for $L = 2, 3$ and 4. Note that the estimation errors obtained with SS-LS PBCI for $L = 4$ are smaller than those of FOSI for $L = 4$ and 3. Furthermore, for low SNR values, the performance provided by the SS-LS PBCI algorithm for channels with $L = 4$ is close to that obtained with FOSI for channels with $L = 2$. We can therefore conclude that, increasing the channel delay spread, the SS-LS PBCI method provides better performance than the two other algorithms, especially in highly noisy situations.

In order to evaluate the effect of the output data sequence length used to estimate the 4th-order cumulants over the performance of the identification algorithms, we plot in Fig. 3 the NMSE against the channel memory for $N = 1000$ and 3000 output data, with SNR = 21 dB. We can conclude that SS-LS PBCI with $N = 1000$ yields better results than TLS and FOSI algorithms with $N = 3000$.

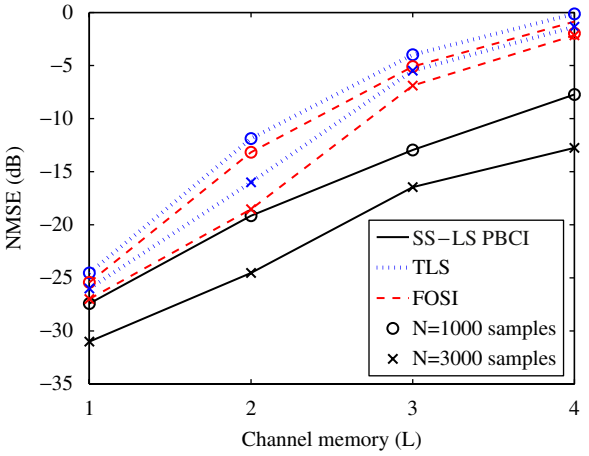

Fig. 3. NMSE × channel memory with SNR = 21 dB.

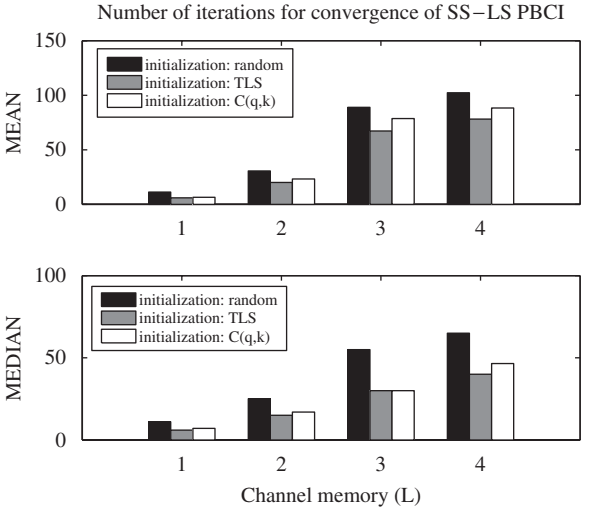

Fig. 4. Convergence analysis for SS-LS PBCI with three different initializations (SNR = 21 dB).

It is interesting to note that the number of iterations required for convergence of the SS-LS PBCI algorithm can be reduced by initializing it with an algebraic solution such as the TLS solution. In Fig. 4 we show the mean and median number of iterations needed for convergence of SS-LS PBCI with SNR = 21 dB using three different initializations: (1) a Gaussian random vector; (2) the TLS solution and (3) the $C(q,k)$ solution [50]. Using either the TLS or the $C(q,k)$ solutions as initialization decreases the number of iterations in comparison with the random initialization. Finally, it is worth to mention that the NMSE performance after convergence remains unchanged, i.e. initialization only affects convergence speed.

7.1.1. Recovery of the input signal

Several equalization approaches exist to recover the input data sequence using the estimated channel. The optimal solution in the minimum mean squared error (MMSE) sense is provided by the Wiener solution. The coefficient vector $\mathbf{w} \in \mathbb{C}^{(K+1)\times 1}$ of the optimal equalizer is given by

$$\mathbf{w}^{(\mathrm{opt})} = (\mathbf{T}^{\mathsf{H}}\mathbf{T} + \sigma_v^2 \mathbf{I}_{(L+1)})^{-1}\mathbf{T}^{\mathsf{H}}\mathbf{s}_d, \tag{49}$$

where $\mathbf{T}$ is a $(K+L+1)\times(L+1)$ Toeplitz matrix built from the channel coefficients as follows:

$$\mathbf{T} = \begin{pmatrix} h_0 & h_1 & \cdots & h_L & 0 & \cdots & 0 \\ 0 & h_0 & \cdots & h_{L-1} & h_L & \cdots & 0 \\ \vdots & \vdots & \ddots & \ddots & \ddots & \ddots & \vdots \\ 0 & 0 & \cdots & h_0 & h_1 & \cdots & h_L \end{pmatrix}^{\mathsf{T}} \tag{50}$$

and $\mathbf{s}_d = \mathbf{e}_d^{(K+L+1)}$, where d represents the equalization delay, usually chosen as $d = (K+L+1)/2$ if $K+L$ is odd or $d = (K+L+2)/2$ if $K+L$ is even.

The input signal is recovered as follows:

$$\hat{s}(n) = \sum_{k=0}^{K} w_k^{(\mathrm{opt})} y(n-k). \tag{51}$$

In Fig. 5, we present the performance of SS-LS PBCI and FOSI algorithms in terms of the symbol error rate (SER) for channels with $L = 2$ (left) and $L = 3$ (right), and a QPSK modulated input signal. The dotted lines represent the results obtained with the optimal MMSE filter assuming perfect knowledge of the channel. For a target SER of 10^{-3}, with $L = 2$, SS-LS PBCI provides a gain of about 5 dB in SNR with respect to FOSI. For $L = 3$, despite the expected performance loss of both algorithms, this gain is around 8 dB in SNR for a target SER of 2×10^{-3}.

7.2. MIMO channel identification

In this section, we consider a *quasi-static* transmission scenario where the complex MIMO channel coefficients are drawn from a Rayleigh distribution and are assumed to be time-invariant within the duration of a time-slot composed of N symbol periods. At each new time-slot the channel varies independently. Except otherwise stated, the length of the time-slot is $N = 1000$ symbol periods and the output data samples received in this interval are used to estimate the spatial cumulants. Our results are averaged over 300 time-slots.

In order to evaluate the performance of the proposed Parafac-based blind MIMO channel identification algorithms, we utilize the identification performance index given in [51,52], which is based on the matrix $\mathbf{\Phi}^{\langle p \rangle} = \mathbf{H}^{\#}\hat{\mathbf{H}}_{\langle p \rangle}$, where $\hat{\mathbf{H}}_{\langle p \rangle}$ is the channel estimate after convergence of the

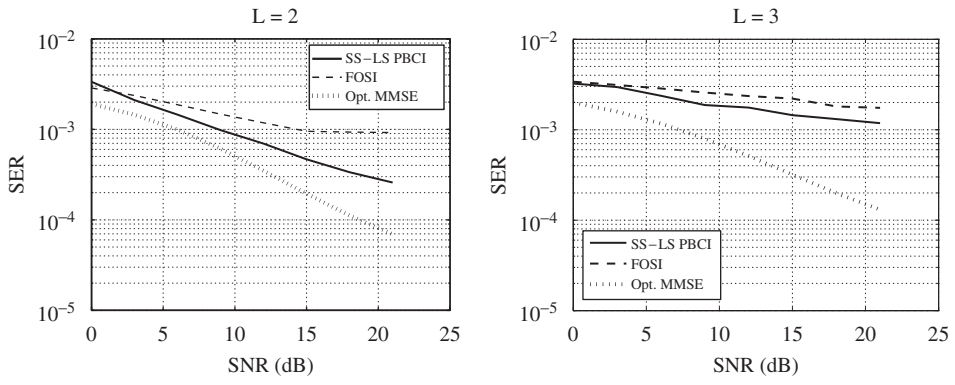

Fig. 5. Symbol error rate (SER) × SNR (QPSK modulation).

experiment $p \in [1, P]$. Since we estimate the channel up to column scaling and permutation, it is easy to conclude that $\mathbf{\Phi}^{\langle p \rangle}$ is a scaled permutation matrix. The identification performance index is computed as follows:

$$\xi(\mathbf{\Phi}^{\langle p \rangle}) \triangleq \frac{1}{2}\left[\left(\sum_i\left(\sum_j \frac{|\phi_{i,j}^{\langle p \rangle}|^2}{\max_\ell |\phi_{i,\ell}^{\langle p \rangle}|^2}\right) - 1\right) + \left(\sum_j\left(\sum_i \frac{|\phi_{i,j}^{\langle p \rangle}|^2}{\max_\ell |\phi_{\ell,j}^{\langle p \rangle}|^2}\right) - 1\right)\right], \quad (52)$$

where $\phi_{i,j}^{\langle p \rangle}$ are the entries of $\mathbf{\Phi}^{\langle p \rangle}$. The performance index $\xi(\cdot)$ equals zero if its matrix argument has the exact structure of a scaled permutation matrix, and small values indicate proximity to the desired solution. In our case, $\xi(\mathbf{\Phi}^{\langle p \rangle})$ tends towards zero when the channel estimate approximates the actual MIMO channel matrix, up to column scaling and permutation. Eq. (52) provides, therefore, a measure of the global level of interference rejection between the estimated channels, irrespective of the trivial ambiguities. In the following figures, we plot the value of the average performance index, i.e. $(1/P)\sum_{p=1}^{P} \xi(\mathbf{\Phi}^{\langle p \rangle})$, where $P = 300$ is the number of time-slots (Monte Carlo simulations).

We first evaluate the PBMCI approach by comparing the proposed algorithms 4D SS-LS and 3D SS-LS with their ALS-based counterparts (QALS and TALS, respectively). Using $M = 3$ sensors, we show in Fig. 6 the average identification performance index computed using (52) in function of the SNR for $Q = 2$ (left) and $Q = 3$ (right) QPSK modulated sources. We can conclude that the methods based on 4th-order tensors (4D SS-LS and QALS) performed better than their 3rd-order versions (3D SS-LS and TALS). As expected, increasing the number of sources degrades the performance, but 4D SS-LS is less affected than the other methods.

In Fig. 7, we show the mean number of iterations needed for convergence of the four algorithms when

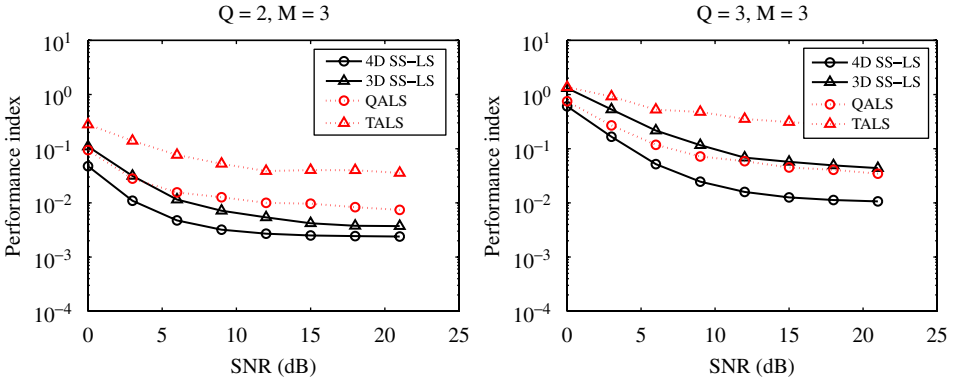

Fig. 6. Average identification performance index × SNR.

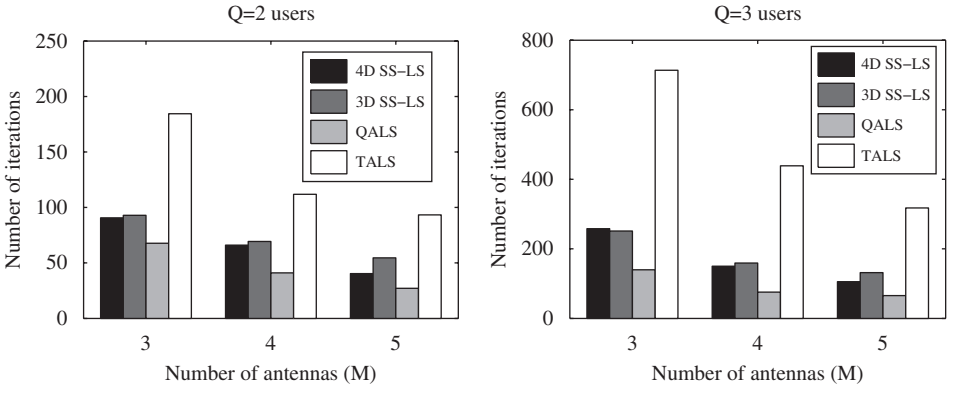

Fig. 7. Mean number of iterations for convergence with SNR = 21 dB.

$Q = 2$ (left) and $Q = 3$ sources (right) with SNR = 21 dB. Although 4D SS-LS takes generally more iterations to converge than QALS, the former one is a more attractive solution due to its smaller computational complexity, since it involves only one LS minimization per iteration, instead of four. Note that increasing the number of users for a given number of antennas significantly increases the number of iterations needed for convergence. As expected, the methods based on the 4th-order tensor converge faster than those based on the 3rd-order one. Finally, we observe that the algorithms take more iterations to converge when the number of antennas decreases, i.e. when the spatial diversity decreases.

As recent papers have compared new approaches with several classical blind channel identification algorithms (cf. see [13]) we compare our methods with some of the most performing algorithms reported in the literature. In the sequel, we show some simulation results comparing the identification performance of the 4D SS-LS PBMCI with the classical JADE [9] algorithm, the FOOBI [14] and the ICAR [13] methods. The SOBI algorithm [10] and its counterpart to high-order cumulants (FOBIUM [49]) have not been considered because they are theoretically unable to deal with sources that have similar trispectra.

For $Q = 2$ users and $M = 3$ antennas, Fig. 8 (left) shows that the 4D SS-LS PBMCI performance is close to that of the ICAR and FOOBI algorithms. Note that JADE degrades when the noise power increases, becoming less performing than the other methods for SNR lower than 12 dB. For $Q = 3$ sources and $M = 3$ antennas, Fig. 8 (right) indicates that our approach performs better than the other tested algorithms. We have also simulated the case of $M = 5$ antennas and observed improved results for all the algorithms. For instance, with $M = 5$ and $Q = 3$, JADE becomes better than 4D SS-LS for SNR $\geqslant$ 7.5 dB. Besides, ICAR and FOOBI also take advantage of the additional degrees of freedom and both attain nearly the same performance as 4D SS-LS. In these scenarii, 4D SS-LS seems to be a very interesting solution, especially when noise becomes important and the ratio M/Q is close to one.

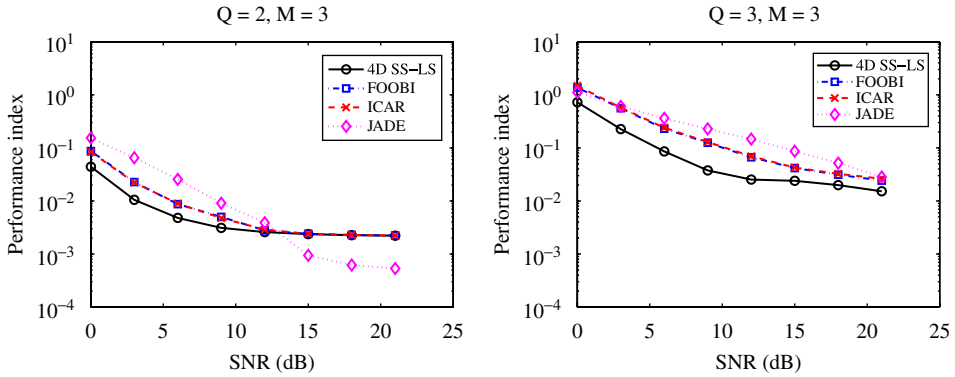

Fig. 8. Comparison with other algorithms.

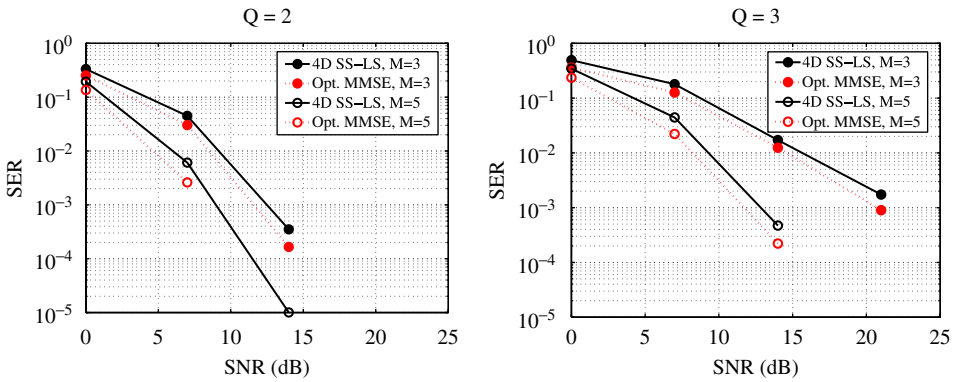

Fig. 9. SER vs. SNR.

Finally, concerning the recovery of the source signals, Fig. 9 illustrates the performance of the 4D SS-LS PBMCI algorithm in terms of the average SER per user, for $Q = 2$ and 3 users. The source symbols were recovered using a *semi-blind* MMSE filter built from the estimated MIMO channel matrices. A few pilot symbols were used in order to eliminate scaling (phase) and permutation ambiguities. The results are compared with those obtained with the optimal MMSE receiver using perfect knowledge of the channel. Note that, for $Q = 2$ as well as for $Q = 3$, the performance of 4D SS-LS is quite close to the optimal MMSE reference. The average SER for $Q = 2$ users presents the same global behavior as that for $Q = 3$ users, except for a vertical shift in the curves, indicating an expected performance loss due to an increase of the number of users.

8. Conclusions and perspectives

A new blind FIR SISO channel identification algorithm has been presented using the Parafac decomposition of a 3rd-order tensor formed of 4th-order output cumulants. The so-called SS-LS PBCI algorithm relies on an iterative single-step LS minimization. The Parafac decomposition fully exploits the three-dimensional nature of the cumulant tensor and has the advantage of avoiding the pre-whitening step needed by the joint-diagonalization based methods. Uniqueness and convergence issues have been addressed. Computer simulations show that our approach provides better estimation performance than both the TLS solution and the FOSI algorithm, which is based on a simultaneous matrix diagonalization. Furthermore, the convergence of the PBCI algorithm can be accelerated when it is initialized with the TLS solution.

We have also addressed the problem of blind MIMO channel (mixture) identification in the context of a multiuser system characterized by instantaneous complex-valued channels. We have presented an iterative SS-LS identification algorithm based on the Parafac decomposition of a 4th-order tensor composed of 4th-order spatial output cumulants. Quadrilinear and trilinear ALS solutions have also been described and compared with the SS-LS method. We have established uniqueness conditions limiting the maximum allowed number of users and showing that, under certain conditions, our algorithm can identify underdetermined mixtures. Computer simulations have been presented assessing the performance of the proposed algorithm and showing that using the SS approach can be of great interest in reducing computational complexity of tensor-based MIMO channel identification algorithms.

Some works deriving from the ideas presented in this paper are considered for the near future, including the use of the SS-LS approach for the estimation of multipath parameters in wireless channels. Preliminary studies have been done on the estimation of the direction-of-arrival (DOA) of the sources placed at the far-field of an antenna array, exploiting specific properties of the MIMO channel matrix. Extending this solution to the case of convolutive MIMO channels is also envisaged in order to treat multipath channels.

References

[1] J.M. Mendel, Tutorial on higher-order statistics (spectra) in signal processing and systems theory: theoretical results and some applications, Proceedings of IEEE 79 (3) (March 1991) 278–305.

[2] C.L. Nikias, J.M. Mendel, Signal processing with higher-order spectra, IEEE Signal Process. Mag. 10 (3) (July 1993) 10–37.

[3] G.B. Giannakis, J.M. Mendel, Identification of non-minimum phase systems using higher-order statistics, IEEE Trans. Acoust. Speech Signal Process. 37 (March 1989) 360–377.

[4] B. Friedlander, B. Porat, Adaptive IIR algorithms based on high-order statistics, IEEE Trans. Acoust. Speech Signal Process. 37 (1989) 485–495.

[5] P. Comon, MA identification using fourth order cumulants, Signal Process. Elsevier 26 (3) (March 1992) 381–388.

[6] P. McCullagh, Tensor methods in statistics, in: Monographs on Statistics and Applied Probability, Chapman and Hall, London, 1987.

[7] J.-F. Cardoso, Eigen-structure of the fourth-order cumulant tensor with application to the blind source separation problem, in: Proceedings of ICASSP, Albuquerque, NM, USA, 1990, pp. 2655–2658.

[8] J.-F. Cardoso, Super-symmetric decomposition of the fourth-order cumulant tensor. Blind identification of more sources than sensors, in: Proceedings of ICASSP, Toronto, Canada, 1991, pp. 3109–3112.

[9] J.-F. Cardoso, A. Souloumiac, Blind beamforming for non Gaussian signals, IEE Proc.-F 140 (6) (December 1993) 362–370.

[10] A. Belouchrani, K. Abed-Meraim, J.-F. Cardoso, E. Moulines, A blind source separation technique using second-order statistics, IEEE Trans. Signal Process. 45 (2) (February 1997) 434–444.

[11] A. Belouchrani, B. Derras, An efficient fourth-order system identification FOSI algorithm utilizing the joint diagonalization procedure, in: Proceedings of the 10-th IEEE Workshop on Statistical Signal and Array Processing, Pocono Manor, Pennsylvania, USA, August 2000, pp. 621–625.

[12] L. De Lathauwer, B. De Moor, J. Vandewalle, J.-F. Cardoso, Independent component analysis of largely underdetermined mixtures, in: Proceedings of the Fourth International Symposium on Independent Component Analysis and Blind Signal Separation (ICA 2003), Nara, Japan, April 2003, pp. 29–34.
[13] L. Albera, A. Ferréol, P. Chevalier, P. Comon, ICAR: a tool for blind source separation using fourth-order statistics only, IEEE Trans. Signal Process. 53 (10) (October 2005) 3633–3643.
[14] L. De Lathauwer, J. Castaing, J.-F. Cardoso, Fourth-order cumulant-based blind identification of uderdetermined mixtures, IEEE Trans. Signal Process. 55 (6) (June 2007) 2965–2973.
[15] P. Comon, Independent component analysis, a new concept?, Signal Process. Elsevier 3 (36) (1994) 287–314.
[16] E. Moreau, A generalization of joint-diagonalization criteria for source separation, IEEE Trans. Signal Process. 49 (3) (March 2001) 530–541.
[17] L. De Lathauwer, B. De Moor, J. Vandewalle, Independent component analysis and (simultaneous) third-order tensor diagonalization, IEEE Trans. Signal Process. 49 (10) (October 2001) 2262–2271.
[18] L. De Lathauwer, B. De Moor, J. Vandewalle, Computation of the canonical decomposition by means of a simultaneous generalized Schur decompositition, SIAM J. Matrix Anal. Appl. 6 (2) (2004) 295–327.
[19] R.A. Harshman, Foundations of the PARAFAC procedure: model and conditions for an "explanatory" multi-mode factor analysis, UCLA Working Papers in Phonetics 16 (1) (1970) 1–84.
[20] L. De Lathauwer, B. De Moor, J. Vandewalle, Independent component analysis based on higher-order statistics only, in: Proceedings of the Eighth IEEE SP Workshop on Statistical Signal and Array Processing (SSAP'96), Corfu, Greece, June 1996, pp. 356–359.
[21] L. De Lathauwer, B. De Moor, J. Vandewalle, Blind source separation by simultaneous third-order tensor diagonalization, in: Proceedings of the Eighth European Signal Processing Conference (EUSIPCO'96), Trieste, Italy, September 1996, pp. 2089–2092.
[22] J.B. Kruskal, Three way arrays: rank and uniqueness of trilinear decompositions with applications to arithmetic complexity and statistics, Linear Algebra Appl. 18 (1977) 95–138.
[23] P. Comon, Blind identification and source separation in 2×3 under-determined mixtures, IEEE Trans. Signal Process. 52 (1) (2004) 11–22.
[24] L. Albera, A. Ferréol, P. Comon, P. Chevalier, Blind identification of overcomplete mixtures of sources (BIOME), Linear Algebra Appl. 391C (November 2004) 3–30.
[25] P. Chevalier, A. Ferréol, On the virtual array concept for the fourth order direction finding problem, IEEE Trans. Signal Process. 47 (9) (September 1999) 2592–2595.
[26] P. Chevalier, L. Albera, A. Ferréol, P. Comon, On the virtual array concept for higher order array processing, IEEE Trans. Signal Process. 53 (4) (April 2005) 1254–1271.
[27] P. Comon, M. Rajih, Blind identification of under-determined mixtures based on the characteristic function, Signal Process. Elsevier 86 (9) (September 2006) 2271–2281.
[28] B. Chen, A. Petropulu, Frequency domain blind MIMO system identification based on second- and higher order statistics, IEEE Trans. Signal Process. 49 (8) (August 2001) 1677–1688.
[29] Y. Yu, A.P. Petropulu, Robust PARAFAC based blind estimation of MIMO systems with possibly more inputs than outputs, in: Proceedings of the ICASSP, Toulouse, France, 2006, pp. 133–136.
[30] T. Acar, Y. Yu, A.P. Petropulu, Blind MIMO system estimation based on PARAFAC decomposition of higher order output tensors, IEEE Trans. Signal Process. 54 (11) (November 2006) 4156–4168.
[31] Y. Yu, A.P. Petropulu, PARAFAC based blind estimation of possibly under-determined convolutive MIMO systems, IEEE Trans. Signal Process, 2008, to appear.
[32] L. De Lathauwer, A link between the canonical decomposition in multilinear algebra and simultaneous matrix diagonalization, SIAM J. Matrix Anal. Appl. 28 (3) (2006) 642–666.
[33] L. Albera, A. Ferréol, P. Comon, P. Chevalier, Sixth order blind identification of under-determined mixtures (BIRTH) of sources, in: Proceedings of the ICA'03 4th International Symposium on Independent Component Analysis and Blind Signal Separation, Nara, Japan, April 2003, pp. 909–914.
[34] G. Favier, Calcul Matriciel et Tensoriel avec Applications à l'Automatique et au Traitement du Signal, Under preparation, in french, 2007.
[35] J.W. Brewer, Kronecker products and matrix calculus in system theory, IEEE Trans. Circuits Systems 25 (9) (1978) 772–781.
[36] R. Bro, PARAFAC. Tutorial and applications, Elsevier Chemometrics and Intelligent Laboratory Systems 38 (1997) 149–171.
[37] N.D. Sidiropoulos, R. Bro, On the uniqueness of multilinear decomposition of N-way arrays, J. Chemometrics (14) (May 2000) 229–239.
[38] N.D. Sidiropoulos, R. Bro, G.B. Giannakis, Parallel factor analysis in sensor array processing, IEEE Trans. Signal Process. 48 (8) (August 2000) 2377–2388.
[39] A.L.F. de Almeida, G. Favier, J.C.M. Mota, PARAFAC-based unified tensor modeling of wireless communication systems with application to blind multiuser equalization, Signal Process. Elsevier 87 (2) (February 2007) 337–351.
[40] R.A. Harshman, M.E. Lundy, The PARAFAC model for three-way factor analysis and multidimensional scaling, in: H.G. Law, C.W. Snyder, J. Hattie Jr., R.P. McDonald (Eds.), Research Methods for Multimode Data Analysis, New York, Praeger, 1984, pp. 122–215.
[41] X. Liu, N.D. Sidiropoulos, Cramér-Rao bounds for low-rank decomposition of multidimensional arrays, IEEE Trans. Signal Process. 49 (2001) 2074–2086.
[42] A. Smilde, R. Bro, P. Geladi, Multi-way Analysis with Applications in the Chemical Sciences, Wiley, New York, 2004.
[43] D.R. Brillinger, M. Rosenblatt, Computation and interpretation of kth-order spectra, in: B. Harris (Ed.), Spectral Analysis of Time Series, Wiley, New York, USA, 1967, pp. 189–232.
[44] E. Moreau, J.-C. Pesquet, Generalized contrasts for multichannel blind deconvolution of linear systems, IEEE Signal Process. Lett. 4 (6) (June 1997) 182–183.
[45] J.C. Pesquet, M. Castella, A.P. Petropulu, Family of frequency and time-domain contrasts for blind separation

of convolutive mixtures of temporally dependent signals, IEEE Trans. Signal Process. 53 (1) (January 2005) 107–120.

[46] C.E.R. Fernandes, G. Favier, J.C.M. Mota, Parafac-based blind channel identification using 4th-order cumulants, in: Proceedings of VI International Telecommunications Symposium (ITS2006), Fortaleza, Brazil, September 2006.

[47] C.E.R. Fernandes, G. Favier, J.C.M. Mota, Tensor-based blind channel identification, in: Proceedings of IEEE International Conference on Communications (ICC 2007), Glasgow, Scotland, UK, June 2007, pp. 2728–2732.

[48] N.D. Sidiropoulos, X. Liu, Identifiability results for blind beamforming in incoherent multipath with small delay spread, IEEE Trans. Signal Process. 49 (1) (January 2001) 228–236.

[49] A. Ferréol, L. Albera, P. Chevalier, Fourth order blind identification of underdetermined mixtures of sources (FOBIUM), IEEE Trans. Signal Process. 53 (5) (May 2005) 1640–1653.

[50] G.B. Giannakis, Cumulants: a powerful tool in signal processing, Proceedings of IEEE 75 (9) (September 1987) 1333–1334.

[51] E. Moreau, O. Macchi, A one stage self-adaptive algorithm for source separation, in: Proceedings of ICASSP, vol. III, Adelaide, Australia, April 1994, pp. 49–52.

[52] E. Moreau, O. Macchi, High order contrasts for self-adaptive source separation, Int. J. Adaptive Control Signal Process. 10 (1) (January 1996) 19–46.